



Higgs properties at ATLAS

Magda Chelstowska
University of Michigan

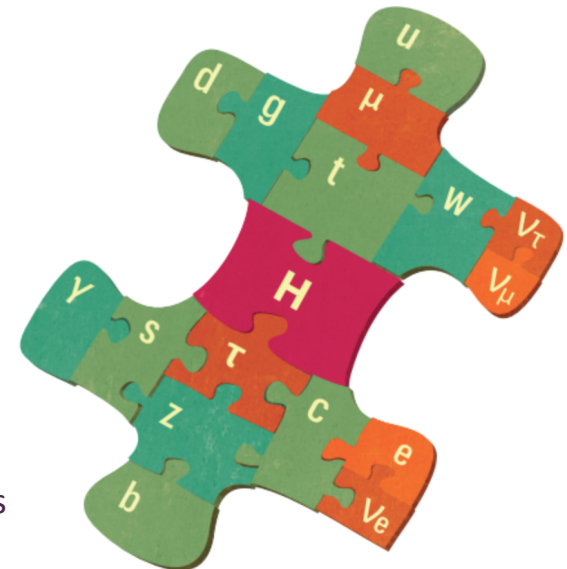
Les Rencontres de Physique de la Vallée d'Aoste
La Thuile

Outline

1. Higgs decay modes (brief overview):

1. $H \rightarrow \gamma\gamma$
2. $H \rightarrow ZZ^* \rightarrow 4l$
3. $H \rightarrow WW^* \rightarrow llvv$
4. $t\bar{t}H(\gamma\gamma, bb)$

Fermion channels ($\tau\tau$, bb and $\mu\mu$)
covered in the talk by Dimitris Varouchas



2. Higgs properties:

1. Mass
2. Spin/CP
3. Couplings combination



The Nobel Prize in Physics 2013



Photo: Pnicolet via
Wikimedia Commons
François Englert

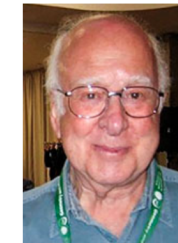


Photo: G-M Greuel via
Wikimedia Commons
Peter W. Higgs

The Nobel Prize in Physics 2013 was awarded jointly to François Englert and Peter W. Higgs "for the theoretical discovery of a mechanism that contributes to our understanding of the origin of mass of subatomic particles, and which recently was confirmed through the discovery of the predicted fundamental particle, by the ATLAS and CMS experiments at CERN's Large Hadron Collider"

Higgs decay modes

Public notes:

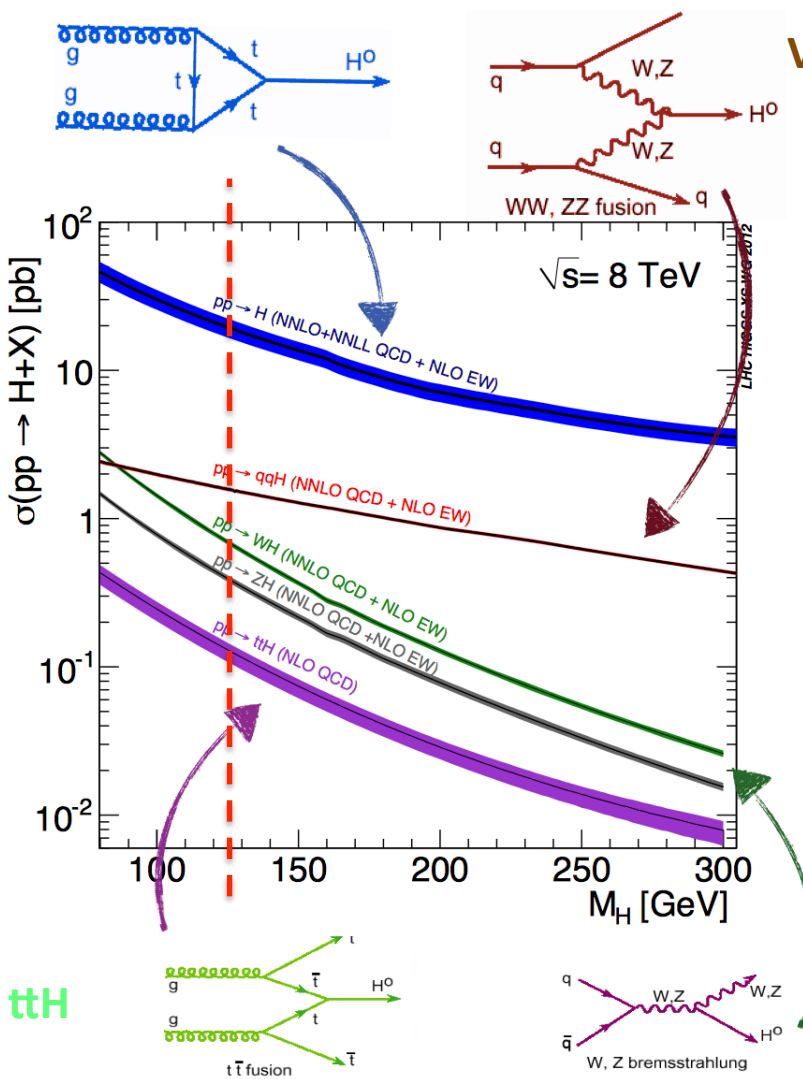
- $\gamma\gamma$ - ATLAS-CONF-2013-012
- ZZ – ATLAS-CONF-2013-013
- WW – ATLAS-CONF-2013-030
- $t\bar{t}H$, bb – ATLAS-CONF-2012-135
- $t\bar{t}H$, $\gamma\gamma$ – ATLAS-CONF-2013-080

Papers ($\gamma\gamma$, ZZ^* and WW^*):

- Couplings – PLB 726 (p. 88-119)
arXiv 1307.1427
- Spin – PLB 726 (p. 120-144)
arXiv 1307.1432

Production and decay modes

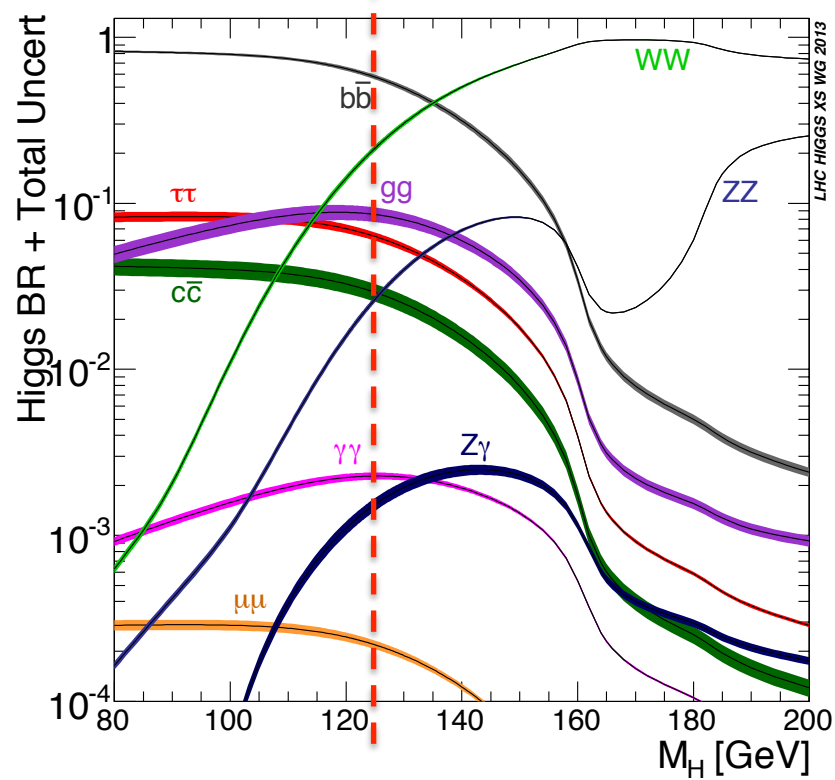
ggF



VBF

WH/ZH

- **WW:** broad sensitivity, different backgrounds
- **$b\bar{b}, \tau\tau$:** fermion couplings, challenging backgrounds
- **ZZ:** very clean, low statistics
- **$\gamma\gamma$:** simple final state, low BR



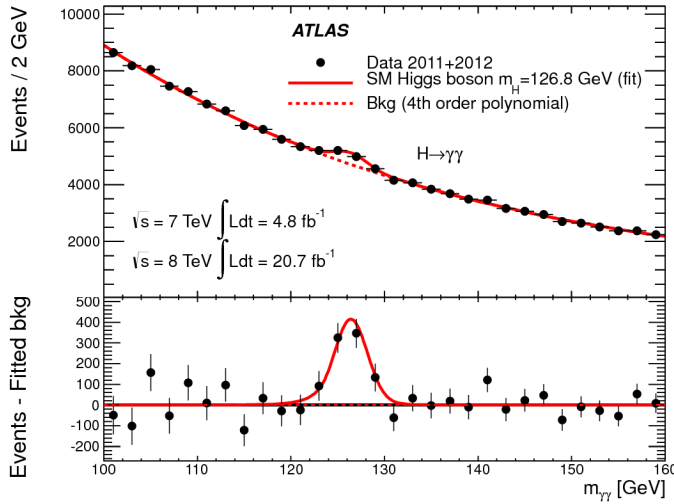
Full Run I data (Moriond2013)
 $\sim 21\text{fb}^{-1}$ 8 TeV and $\sim 5\text{fb}^{-1}$ 7 TeV

$H \rightarrow \gamma\gamma$

Simple selection –
 two high- E_T (30,40 GeV) isolated photons.

14 different categories:

- Increase the sensitivity
 (S/B, mass resolution)
- Separate the production modes
 (ggF/VBF/VH)

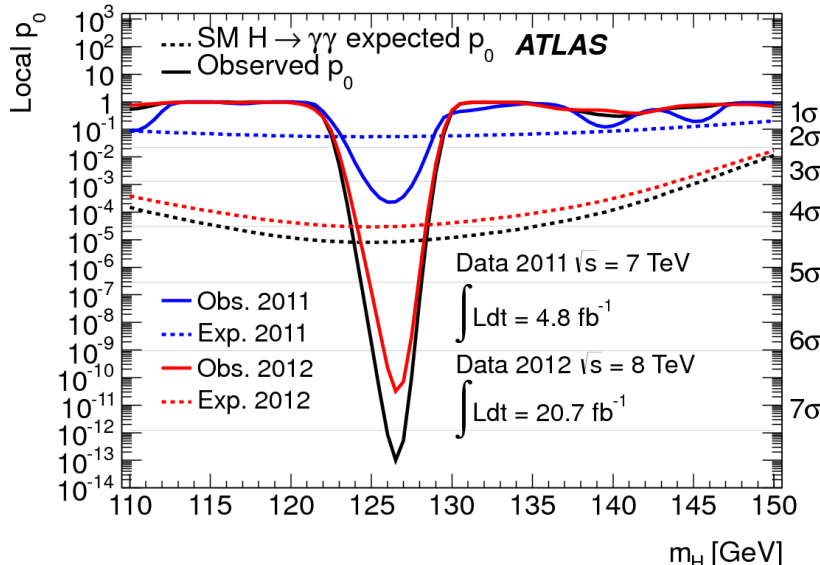


Signal extracted by fit to $m_{\gamma\gamma}$

2/27/14

M.Chelstowska

$$\mu = \sigma \times \text{Br} / \sigma_{\text{SM}} \times \text{Br}_{\text{SM}}$$



	Observed	Expected
7+8 TeV	7.4σ	4.1σ

@ 126.8 GeV, best-fit $\mu = 1.65^{+0.34}_{-0.30}$

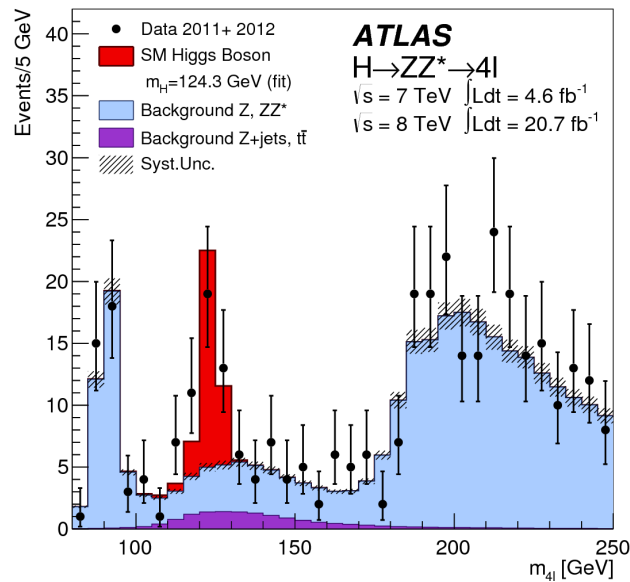
Background extrapolated from sidebands in data: $\gamma\gamma$, γ -jet and jet-jet

Full Run I data (Moriond2013)
 $\sim 21\text{fb}^{-1}$ 8 TeV and $\sim 5\text{fb}^{-1}$ 7 TeV

$H \rightarrow ZZ^* \rightarrow 4l$

4lepton selection: 2 pairs of OS leptons
 $(p_T > 20, 15, 10, 7(\text{e})/6(\mu) \text{ GeV})$

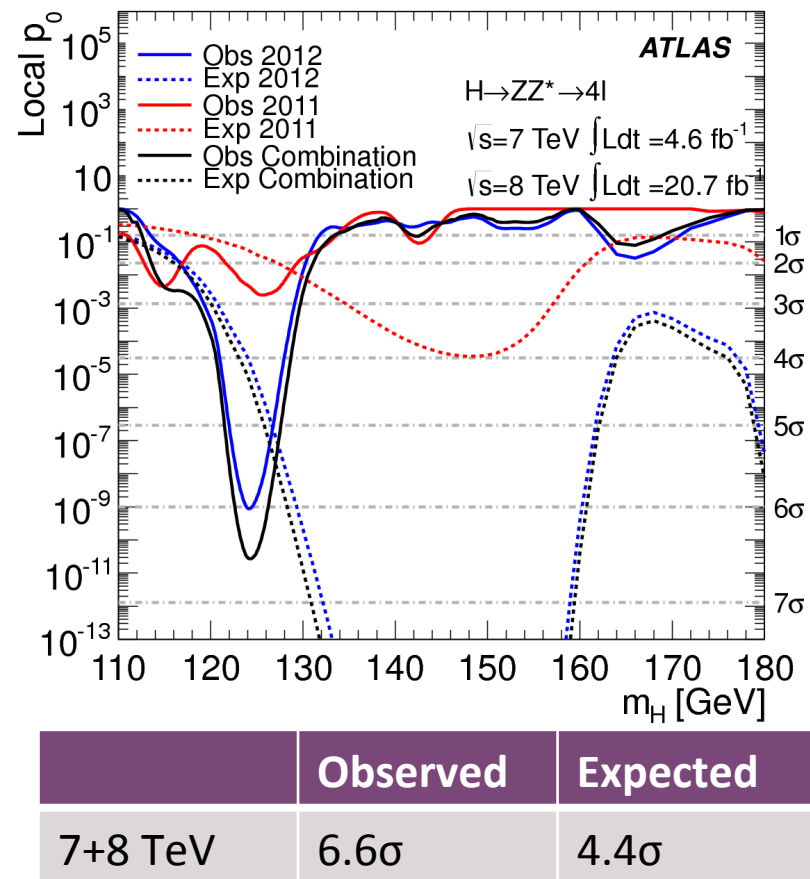
Events are split into 3 categories based on their production mode: ggF, VBF and VH



Signal extracted by fit to m_{4l}

2/27/14

M.Chelstowska



@ 124.3 GeV, best-fit $\mu = 1.7^{+0.5}_{-0.4}$

Background (ZZ , $Z+\text{jets}$, $t\bar{t}$) estimated from control regions, data or MC

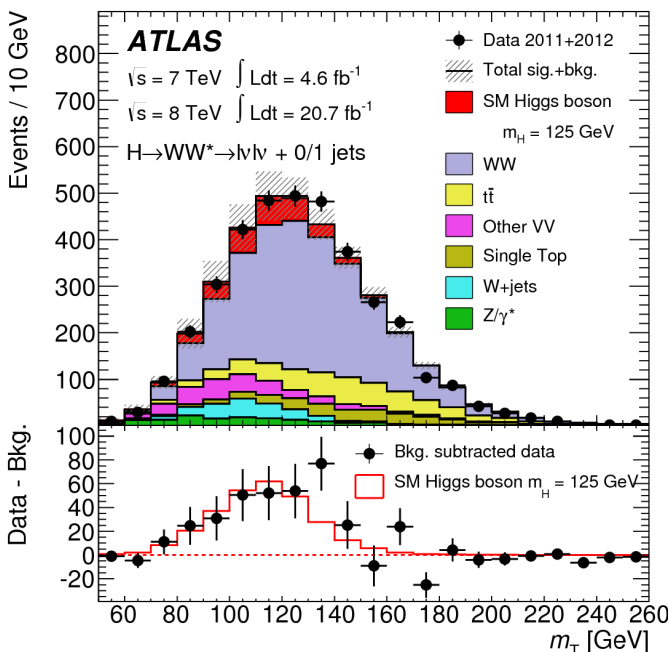
Full Run I data (Moriond2013)

$\sim 21\text{fb}^{-1}$ 8 TeV and $\sim 5\text{fb}^{-1}$ 7 TeV

$H \rightarrow WW^* \rightarrow l\nu l\nu$

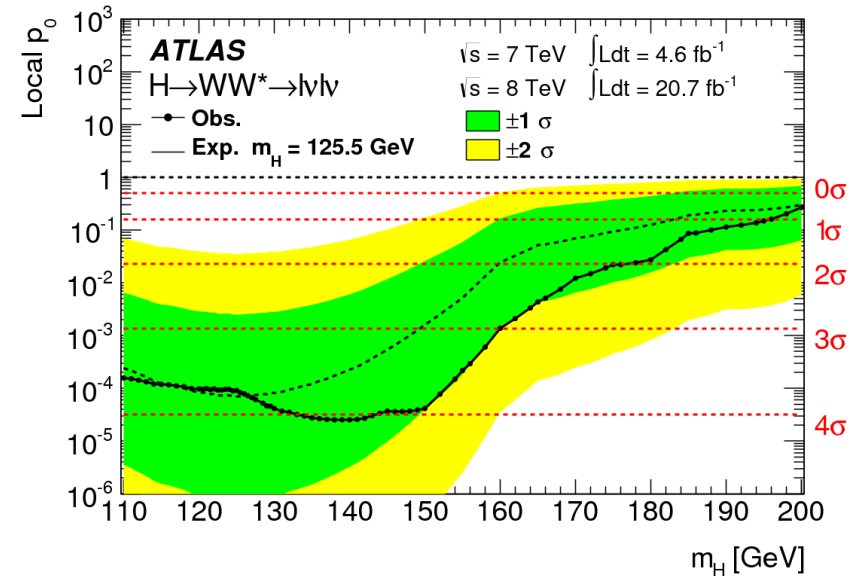
2 OS well isolated leptons with large missing transverse momentum \rightarrow low mass resolution.

Events are split based on the numbers of jets in the final state: ggF / VBF production.



Signal extracted by fit to m_T

2/27/14



	Observed	Expected
7+8 TeV	3.8σ	3.7σ

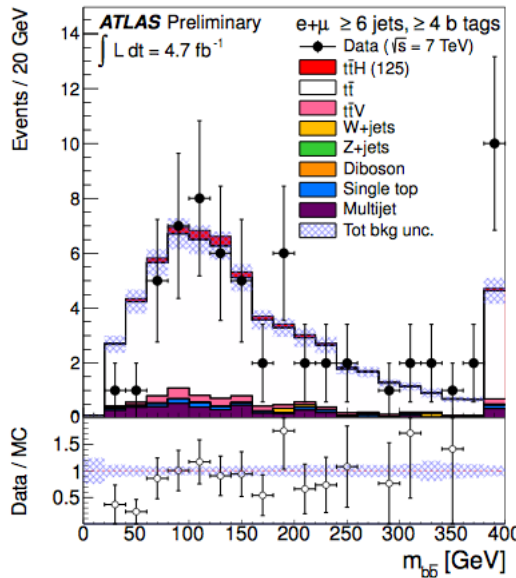
@ 125 GeV, $\mu = 1.01 \pm 0.31$

Background (WW, top, Wjets, Zjets)
 estimated from control regions and data

M.Chelstowska

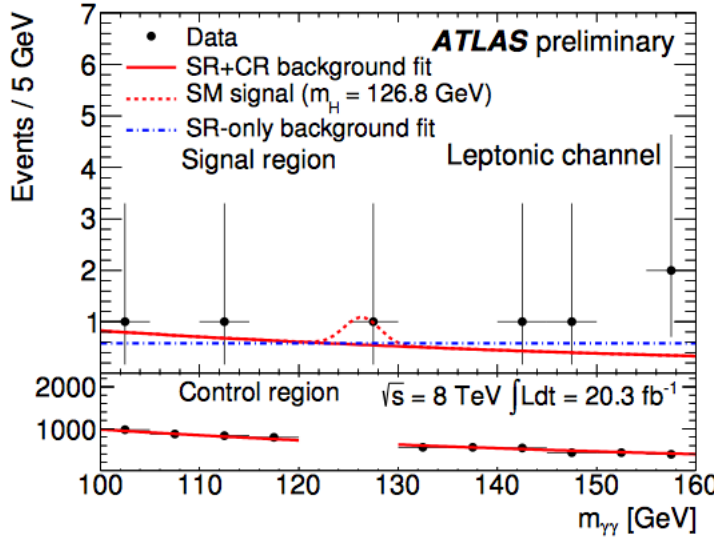
$t\bar{t}H(bb)$ – $\sim 5\text{fb}^{-1}$ 7 TeV data
 $t\bar{t}H(\gamma\gamma)$ – $\sim 20\text{fb}^{-1}$ 8 TeV data

$t\bar{t}H(\gamma\gamma, bb)$



Signal extracted by fit to m_{bb} or H_T (scalar sum of the jet momenta) depending on the categories with varying S/B.

No excess is observed in either of the channels therefore limits are set on the cross section times the branching ratio (wrt the SM expectation) at 95% CL.



	Observed	Expected
$t\bar{t}H, H \rightarrow bb @ 125 \text{ GeV}$	13.1	10.5
$t\bar{t}H, H \rightarrow \gamma\gamma @ 126.8 \text{ GeV}$	5.3	6.4

Signal extracted by fit to $m_{\gamma\gamma}$.

Higgs properties

Public notes:

- Mass – ATLAS-CONF-2013-014
- Couplings – ATLAS-CONF-2013-034
- Spin - ATLAS-CONF-2013-040

Papers ($\gamma\gamma$, ZZ^* and WW^*):

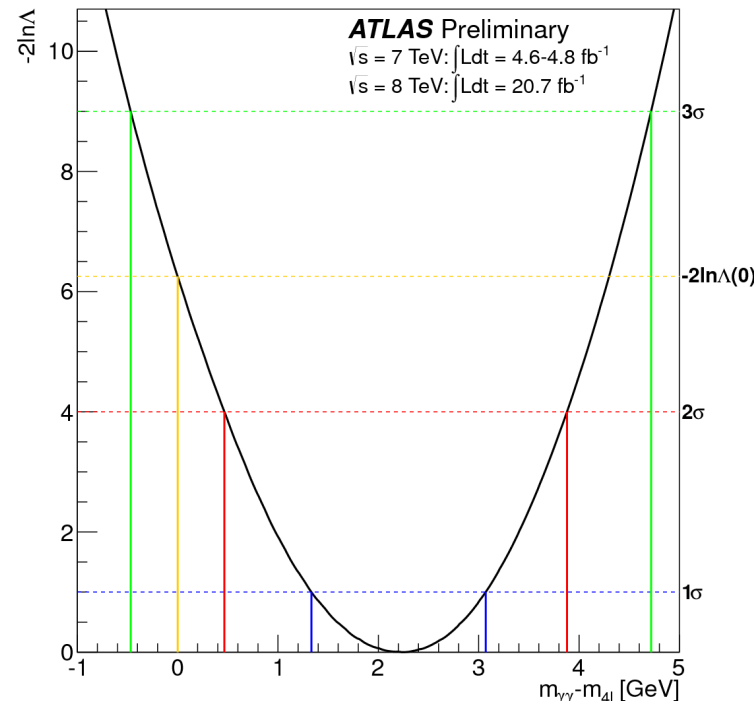
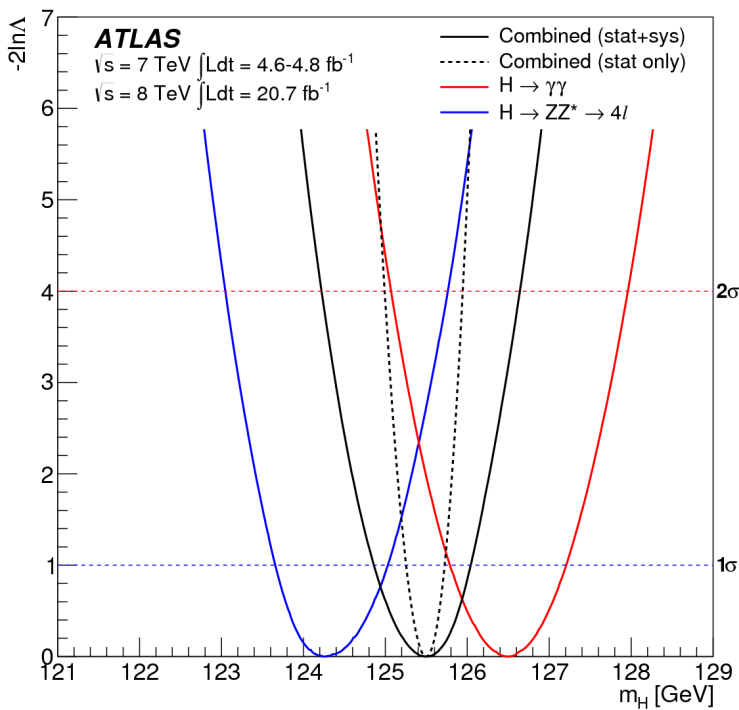
- Couplings – PLB 726 (p. 88-119)
arXiv 1307.1427
- Spin – PLB 726 (p. 120-144)
arXiv 1307.1432

Mass

Higgs boson's mass is extracted from the mass measurements from two channels:

$$\begin{aligned} H \rightarrow \gamma\gamma & \quad 126.8 \pm 0.2 \text{ (stat)} \pm 0.7 \text{ (sys)} \text{ GeV} \\ H \rightarrow ZZ^* \rightarrow 4l & \quad 124.3^{+0.6}_{-0.5} \text{ (stat)}^{+0.5}_{-0.3} \text{ (sys)} \text{ GeV} \end{aligned}$$

$$m_H = 125.5 \pm 0.2 \text{ (stat)}^{+0.5}_{-0.6} \text{ (sys)} \text{ GeV}$$



Mass difference is measured to be:

$$\Delta\hat{m}_H = \hat{m}_H^{\gamma\gamma} - \hat{m}_H^{4\ell} = 2.3^{+0.6}_{-0.7} \text{ (stat)} \pm 0.6 \text{ (sys)} \text{ GeV}$$

It is compatible with $\Delta m_H = 0$ at a level of 2.4σ

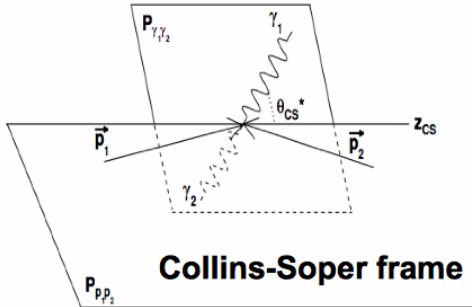
Spin-Parity

SM spin-parity $J^P = 0^+$ hypothesis is compared with alternatives from three channels:
 $H \rightarrow \gamma\gamma$, $H \rightarrow ZZ^*$ and $H \rightarrow WW^*$

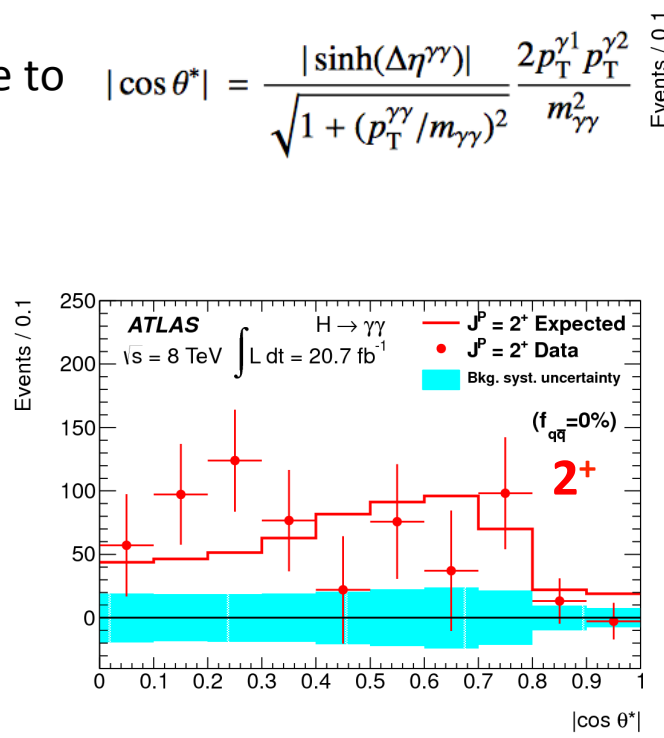
Hypotheses tested are: 0^- , 1^+ , 1^- and 2^+ (graviton-like model with minimal couplings). Spin-1 is strongly disfavored by the observation of the $H \rightarrow \gamma\gamma$ decay since the Landau-Yang theorem forbids the direct decay of an on-shell spin-1 particle into a pair of photons

$H \rightarrow \gamma\gamma$ – $|\cos\theta^*|$ is sensitive to the spin information

θ^* - polar angle of the photons wrt the z-axis of the Collins-Soper frame



$$|\cos\theta^*| = \frac{|\sinh(\Delta\eta_{\gamma\gamma})|}{\sqrt{1 + (p_T^{\gamma\gamma}/m_{\gamma\gamma})^2}} \frac{2p_T^{\gamma 1} p_T^{\gamma 2}}{m_{\gamma\gamma}^2}$$



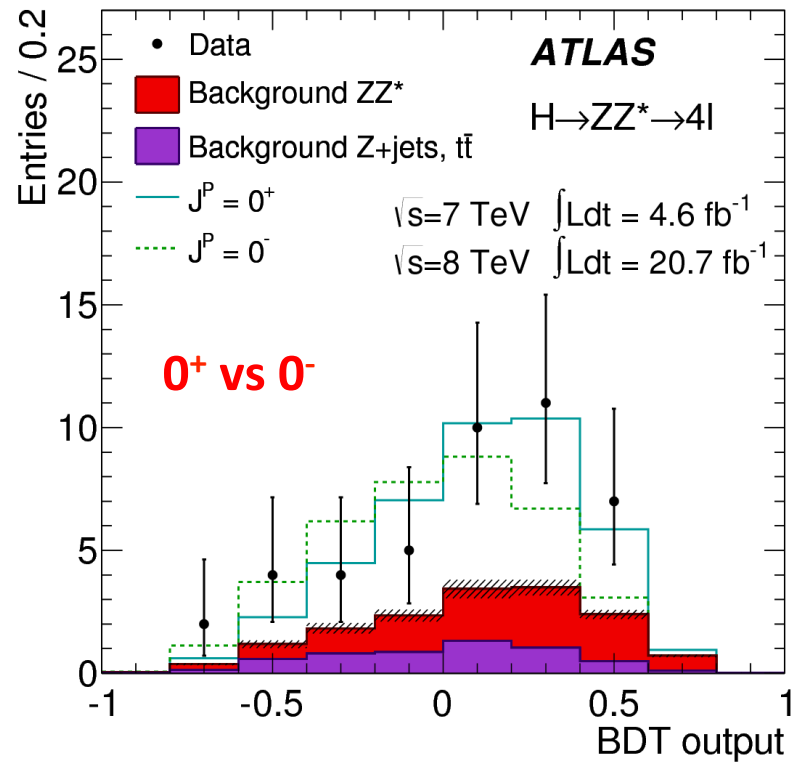
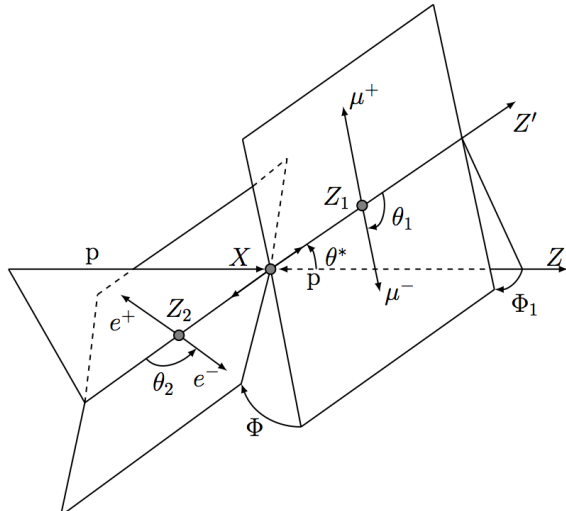
$m_{\gamma\gamma}$ is used to discriminate between signal and background processes

Spin-Parity

SM spin-parity $J^P = 0^+$ hypothesis is compared with alternatives from three channels:
 $H \rightarrow \gamma\gamma$, $H \rightarrow ZZ^*$ and $H \rightarrow WW^*$

Hypotheses tested are: 0^- , 1^+ , 1^- and 2^+ .

$H \rightarrow ZZ^*$ – reconstructed masses of two Z bosons, 1 production and 4 decay angles, serve as inputs to BDT

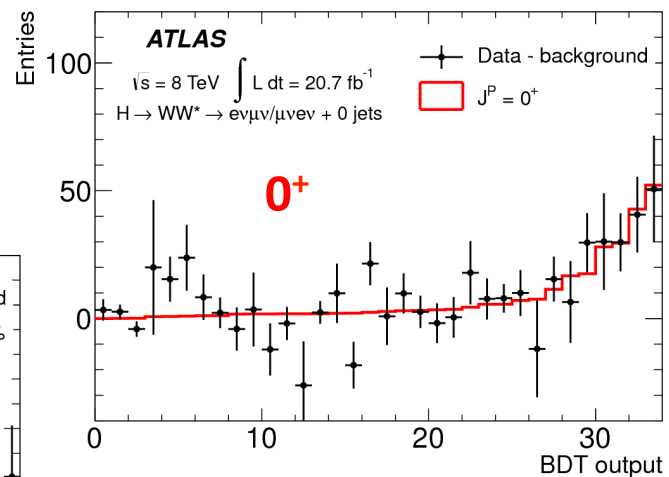
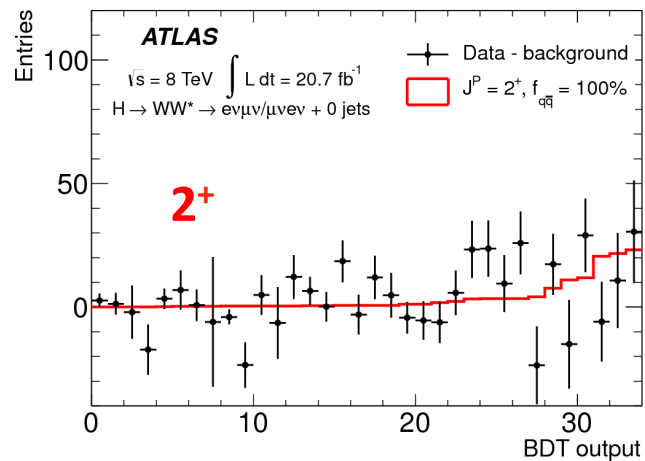
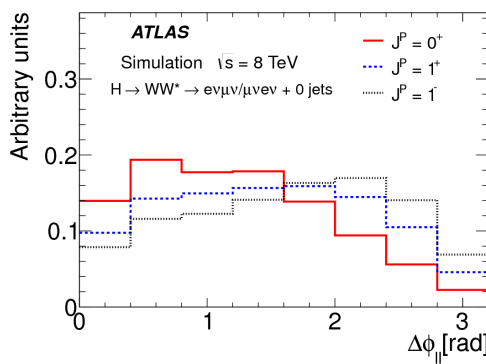


Spin-Parity

SM spin-parity $J^P = 0^+$ hypothesis is compared with alternatives from three channels:
 $H \rightarrow \gamma\gamma$, $H \rightarrow ZZ^*$ and $H \rightarrow WW^*$

Hypotheses tested are: 0^- , 1^+ , 1^- and 2^+ .

$H \rightarrow WW^*$ – $\Delta\Phi(\text{II})$, $m(\text{II})$, $pT(\text{II})$
 and m_T
 serve as inputs to BDT.



Spin-Parity

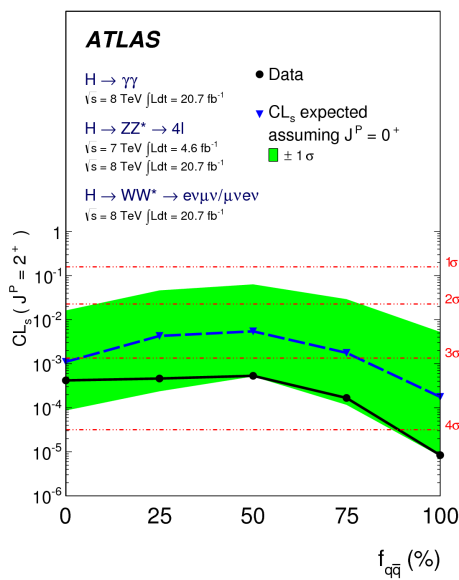
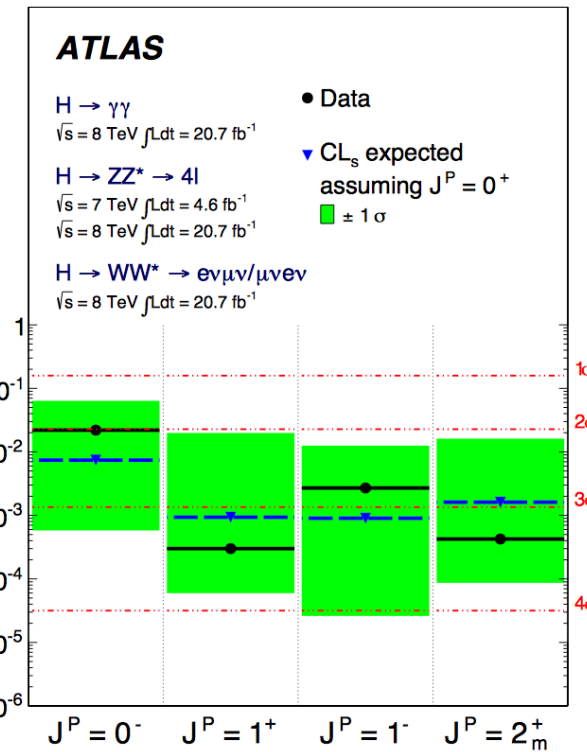
The exclusion of the alternative J_{alt}^P hypothesis in favour of the Standard Model 0^+ hypothesis is evaluated in terms of the corresponding $\text{CL}_s(J_{\text{alt}}^P)$, defined as:

$$\text{CL}_s(J_{\text{alt}}^P) = \frac{p_0(J_{\text{alt}}^P)}{1 - p_0(0^+)} . \quad (3)$$

The exclusion of the alternative hypotheses using CL_s in favor of 0^+ :

J^P	Inputs	$\text{CL} [\%]$
0^-	ZZ	97.8
1^+	ZZ, WW	99.97
1^-	ZZ, WW	99.7
2^+_m	$\gamma\gamma$, ZZ, WW	99.9

2^+_m - assuming 0% f_{qq} fraction



2^+_m hypothesis is tested as a function of the fraction f_{qq}

Inputs to the couplings combination

Higgs Boson Decay	Subsequent Decay	Sub-Channels	$\int L dt$ [fb $^{-1}$]	Ref.
2011 $\sqrt{s} = 7$ TeV				
$H \rightarrow ZZ^{(*)}$	4ℓ	{4e, 2e2 μ , 2 μ 2e, 4 μ , 2-jet VBF, ℓ -tag}	4.6	[8]
$H \rightarrow \gamma\gamma$	–	10 categories $\{p_{Tt} \otimes \eta_\gamma \otimes \text{conversion}\} \oplus \{\text{2-jet VBF}\}$	4.8	[7]
$H \rightarrow WW^{(*)}$	$\ell\nu\ell\nu$	{ee, e μ , μ e, $\mu\mu$ } $\otimes \{\text{0-jet, 1-jet, 2-jet VBF}\}$	4.6	[9]
$H \rightarrow \tau\tau$	$\tau_{\text{lep}}\tau_{\text{lep}}$	{e μ } $\otimes \{\text{0-jet}\} \oplus \{\ell\ell\} \otimes \{\text{1-jet, 2-jet, } p_{T,\tau\tau} > 100 \text{ GeV, VH}\}$	4.6	
	$\tau_{\text{lep}}\tau_{\text{had}}$	{e, μ } $\otimes \{\text{0-jet, 1-jet, } p_{T,\tau\tau} > 100 \text{ GeV, 2-jet}\}$	4.6	[10]
	$\tau_{\text{had}}\tau_{\text{had}}$	{1-jet, 2-jet}	4.6	
$VH \rightarrow Vbb$	$Z \rightarrow \nu\nu$	$E_T^{\text{miss}} \in \{120 - 160, 160 - 200, \geq 200 \text{ GeV}\} \otimes \{\text{2-jet, 3-jet}\}$	4.6	
	$W \rightarrow \ell\nu$	$p_T^W \in \{< 50, 50 - 100, 100 - 150, 150 - 200, \geq 200 \text{ GeV}\}$	4.7	[11]
	$Z \rightarrow \ell\ell$	$p_T^Z \in \{< 50, 50 - 100, 100 - 150, 150 - 200, \geq 200 \text{ GeV}\}$	4.7	
2012 $\sqrt{s} = 8$ TeV				
$H \rightarrow ZZ^{(*)}$	4ℓ	{4e, 2e2 μ , 2 μ 2e, 4 μ , 2-jet VBF, ℓ -tag}}	20.7	[8]
$H \rightarrow \gamma\gamma$	–	14 categories $\{p_{Tt} \otimes \eta_\gamma \otimes \text{conversion}\} \oplus \{\text{2-jet VBF}\} \oplus \{\ell\text{-tag, } E_T^{\text{miss}}\text{-tag, 2-jet VH}\}$	20.7	[7]
$H \rightarrow WW^{(*)}$	$\ell\nu\ell\nu$	{ee, e μ , μ e, $\mu\mu$ } $\otimes \{\text{0-jet, 1-jet, 2-jet VBF}\}$	20.7	[9]
$H \rightarrow \tau\tau$	$\tau_{\text{lep}}\tau_{\text{lep}}$	{ $\ell\ell$ } $\otimes \{\text{1-jet, 2-jet, } p_{T,\tau\tau} > 100 \text{ GeV, VH}\}$	13	
	$\tau_{\text{lep}}\tau_{\text{had}}$	{e, μ } $\otimes \{\text{0-jet, 1-jet, } p_{T,\tau\tau} > 100 \text{ GeV, 2-jet}\}$	13	[10]
	$\tau_{\text{had}}\tau_{\text{had}}$	{1-jet, 2-jet}	13	
$VH \rightarrow Vbb$	$Z \rightarrow \nu\nu$	$E_T^{\text{miss}} \in \{120 - 160, 160 - 200, \geq 200 \text{ GeV}\} \otimes \{\text{2-jet, 3-jet}\}$	13	
	$W \rightarrow \ell\nu$	$p_T^W \in \{< 50, 50 - 100, 100 - 150, 150 - 200, \geq 200 \text{ GeV}\}$	13	[11]
	$Z \rightarrow \ell\ell$	$p_T^Z \in \{< 50, 50 - 100, 100 - 150, 150 - 200, \geq 200 \text{ GeV}\}$	13	

Inputs to the couplings combination

Higgs Boson Decay	Subsequent Decay	Sub-Channels	$\int L dt$ [fb $^{-1}$]	Ref.
2011 $\sqrt{s} = 7$ TeV				
$H \rightarrow ZZ^{(*)}$	4ℓ	{4e, 2e2 μ , 2 μ 2e, 4 μ , 2-jet VBF, ℓ -tag}	4.6	[8]
$H \rightarrow \gamma\gamma$	–	10 categories $\{p_{Tt} \otimes \eta_\gamma \otimes \text{conversion}\} \oplus \{\text{2-jet VBF}\}$	4.8	[7]
$H \rightarrow WW^{(*)}$	$\ell\nu\ell\nu$	{ee, e μ , μ e, $\mu\mu$ } $\otimes \{0\text{-jet}, 1\text{-jet}, 2\text{-jet VBF}\}$	4.6	[9]
$H \rightarrow \tau\tau$	$\tau_{\text{lep}}\tau_{\text{lep}}$	{e μ } $\otimes \{0\text{-jet}\} \oplus \{\ell\ell\} \otimes \{1\text{-jet}, 2\text{-jet}, p_{T,\tau\tau} > 100 \text{ GeV}, VH\}$	4.6	
	$\tau_{\text{lep}}\tau_{\text{had}}$	{e, μ } $\otimes \{0\text{-jet}, 1\text{-jet}, p_{T,\tau\tau} > 100 \text{ GeV}, 2\text{-jet}\}$	4.6	[10]
	$\tau_{\text{had}}\tau_{\text{had}}$	{1-jet, 2-jet}	4.6	
$VH \rightarrow Vbb$	$Z \rightarrow \nu\nu$	$E_T^{\text{miss}} \in \{120 - 160, 160 - 200, \geq 200 \text{ GeV}\} \otimes \{\text{2-jet, 3-jet}\}$	4.6	
	$W \rightarrow \ell\nu$	$p_T^W \in \{< 50, 50 - 100, 100 - 150, 150 - 200, \geq 200 \text{ GeV}\}$	4.7	[11]
	$Z \rightarrow \ell\ell$	$p_T^Z \in \{< 50, 50 - 100, 100 - 150, 150 - 200, \geq 200 \text{ GeV}\}$	4.7	
2012 $\sqrt{s} = 8$ TeV				
$H \rightarrow ZZ^{(*)}$	–	{4e, 2e2 μ , 2 μ 2e, 4 μ , 2-jet VBF, ℓ -tag}}	20.7	[8]
$H \rightarrow \gamma\gamma$	–	14 categories $\{p_{Tt} \otimes \eta_\gamma \otimes \text{conversion}\} \oplus \{\text{2-jet VBF}\} \oplus \{\ell\text{-tag}, E_T^{\text{miss}}\text{-tag}, \text{2-jet VH}\}$	20.7	[7]
$H \rightarrow WW^{(*)}$	$\ell\nu\ell\nu$	{ee, e μ , μ e, $\mu\mu$ } $\otimes \{0\text{-jet}, 1\text{-jet}, 2\text{-jet VBF}\}$	20.7	[9]
$H \rightarrow \tau\tau$	$\tau_{\text{lep}}\tau_{\text{lep}}$	{ $\ell\ell$ } $\otimes \{1\text{-jet}, 2\text{-jet}, p_{T,\tau\tau} > 100 \text{ GeV}, VH\}$	13	
	$\tau_{\text{lep}}\tau_{\text{had}}$	{e, μ } $\otimes \{0\text{-jet}, 1\text{-jet}, p_{T,\tau\tau} > 100 \text{ GeV}, 2\text{-jet}\}$	13	[10]
	$\tau_{\text{had}}\tau_{\text{had}}$	{1-jet, 2-jet}	13	
$VH \rightarrow Vbb$	$Z \rightarrow \nu\nu$	$E_T^{\text{miss}} \in \{120 - 160, 160 - 200, \geq 200 \text{ GeV}\} \otimes \{\text{2-jet, 3-jet}\}$	13	
	$W \rightarrow \ell\nu$	$p_T^W \in \{< 50, 50 - 100, 100 - 150, 150 - 200, \geq 200 \text{ GeV}\}$	13	[11]
	$Z \rightarrow \ell\ell$	$p_T^Z \in \{< 50, 50 - 100, 100 - 150, 150 - 200, \geq 200 \text{ GeV}\}$	13	

Most recent $H \rightarrow bb$ and $H \rightarrow \tau\tau$ results are not included here!!

Signal parametrization

For each analysis category (k , list on the previous slide) the number of signal events is parametrized in terms of scale factors for:

- the cross section $\sigma_{i,SM}$ of each SM Higgs boson production mode i - $\mu_i = \sigma_i / \sigma_{i,SM}$
- the branching ratio $B_{f,SM}$ of the SM Higgs boson decay modes f - $\mu_f = B_f / B_{f,SM}$.

$$n_{\text{signal}}^k = \left(\sum_i \mu_i \sigma_{i,SM} \times A_{if}^k \times \varepsilon_{if}^k \right) \times \mu_f \times B_{f,SM} \times \mathcal{L}^k$$

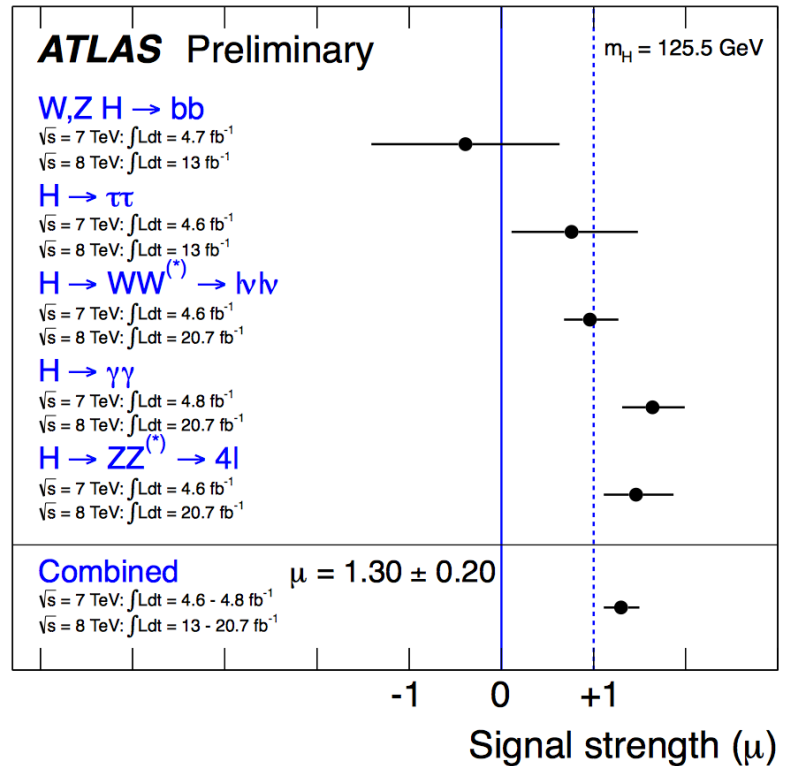
A - detector acceptance
 ε – reconstruction efficiency
 \mathcal{L} – integrated luminosity

- generalizes the dependence on the signal yields from the x-sec and branching fractions
- relationship between the production and decay (specific theory or benchmark) is achieved via a parametrization of $\mu_i, \mu_f \rightarrow f(\kappa)$;

$\mu_i \mu_f$ – the product can be represented by μ_j (or globally by μ , where $\mu=1 \rightarrow$ SM Higgs boson and $\mu=0 \rightarrow$ bkg-only).

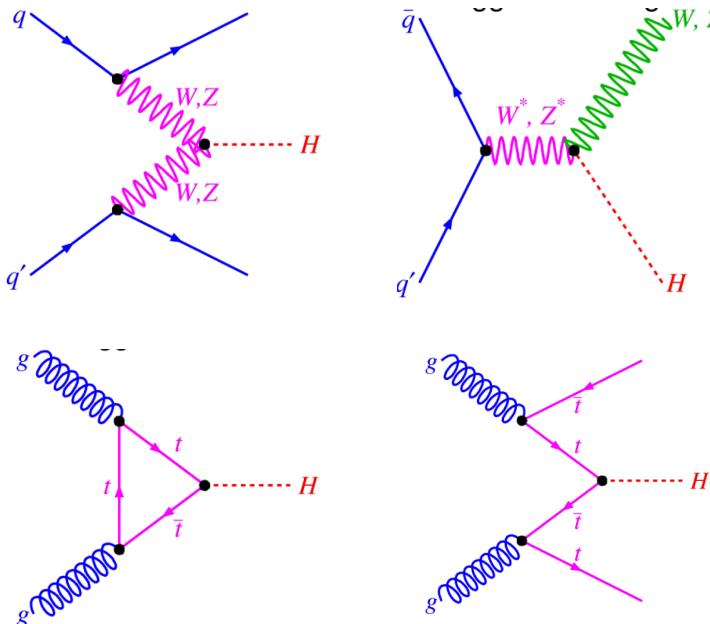
Global signal strength

Higgs Boson Decay	μ ($m_H = 125.5 \text{ GeV}$)
$VH \rightarrow Vbb$	-0.4 ± 1.0
$H \rightarrow \tau\tau$	0.8 ± 0.7
$H \rightarrow WW^{(*)}$	1.0 ± 0.3
$H \rightarrow \gamma\gamma$	1.6 ± 0.3
$H \rightarrow ZZ^{(*)}$	1.5 ± 0.4
Combined	1.30 ± 0.20



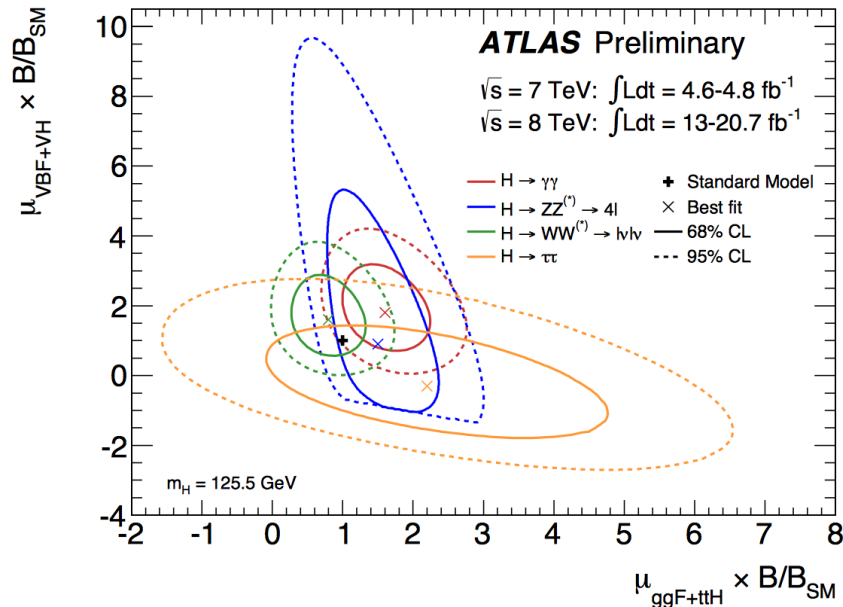
- Individual best-fit μ_i compatible with combined best-fit μ at 13% CL, and with $\mu=1$ at 8% CL
- Combined best-fit μ compatible with $\mu=1$ at 9% CL

Production modes



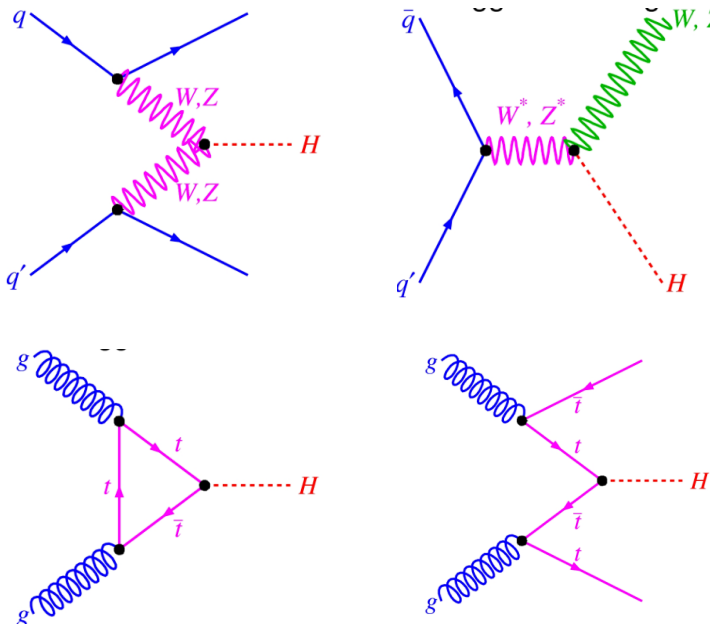
VBF and VH –
W/Z mediated

ggF and ttH –
quark mediated



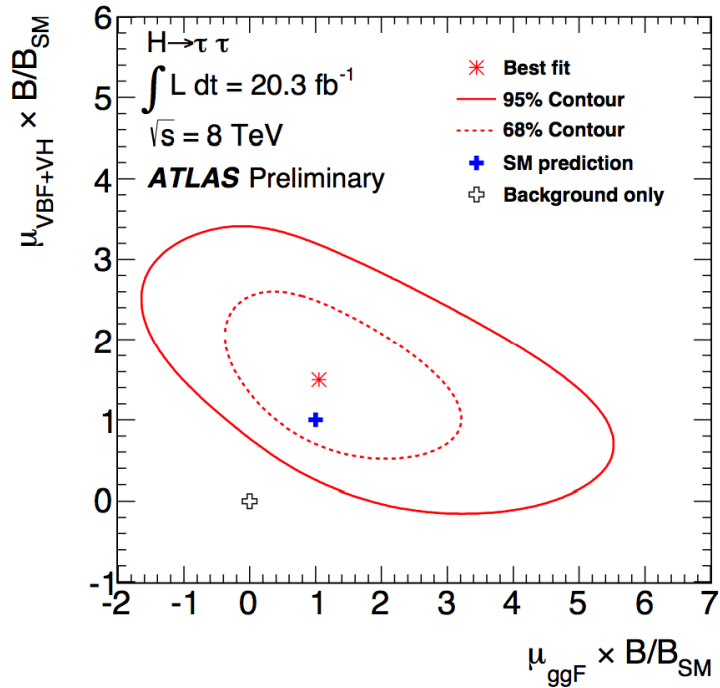
Each $\mu_{\text{ggF+ttH}}$ and $\mu_{\text{VBF+VH}}$ are modified by the branching ratio factors B/B_{SM} , which are different for different final states \rightarrow direct combination of contours is not possible.

Production modes



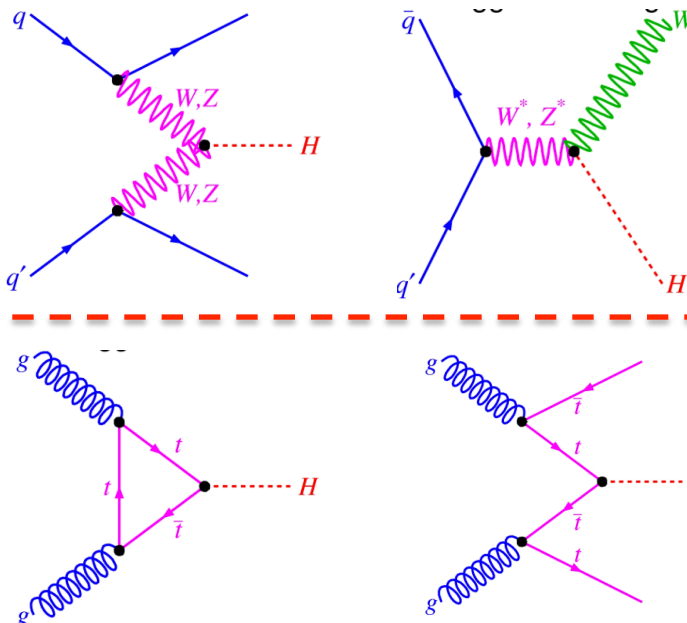
VBF and VH –
W/Z mediated

ggF and ttH –
quark mediated



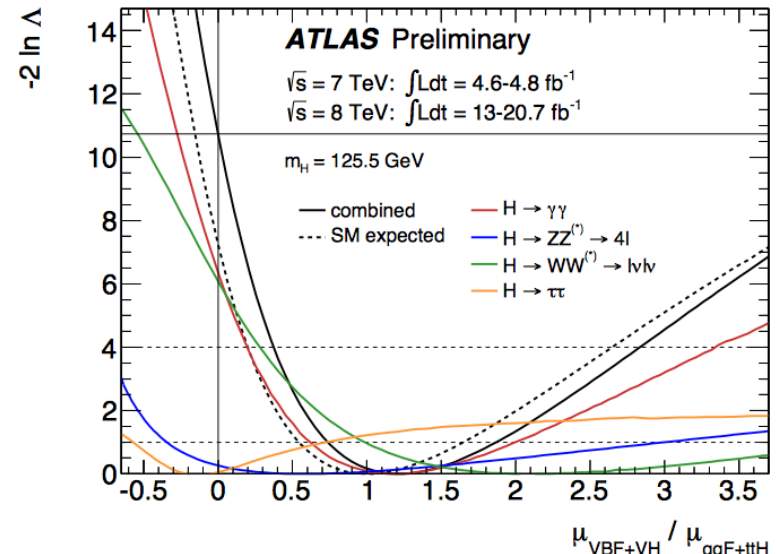
The latest $H \rightarrow \tau\tau$ analysis (as presented in the previous talk) interpreted in the context of $\mu_{ggF+ttH}$ and μ_{VBF+VH} production signal strengths.

Production modes



VBF and VH –
W/Z mediated

ggF and ttH –
quark mediated



$$\mu_{VBF+VH} / \mu_{ggF+t\bar{t}H} = 1.2^{+0.7}_{-0.5}$$

Use the ratio of production modes
(B/B_{SM} cancels) \rightarrow relative
discrimination power between
ggF+ $t\bar{t}H$ and VBF+VH

Compatible with the SM expectation of unity.
 p_0 value of $\mu_{VBF+VH} = 0$ hypothesis is 0.05% \rightarrow
 3.3σ evidence of the vector boson mediated
production.

Coupling fit

For a consistent measurement of Higgs couplings, the production and decay modes cannot be treated independently.

Assumptions:

- 1) The signals observed in different search channels originate from the same resonance. A mass of 125.5 GeV is assumed.
- 2) The width of the Higgs boson is narrow. The predicted rate for a given channel can be decomposed:

$$\sigma \cdot B(i \rightarrow H \rightarrow f) = \frac{\sigma_i \cdot \Gamma_f}{\Gamma_H}$$

- 3) Only modifications of coupling strengths are allowed. The observed state is a CP-even scalar

The coupling scale factors κ_j are defined in such a way that σ_j and Γ_j scale with κ^2 when compared to the SM prediction. For example:

$$\sigma \cdot BR(gg \rightarrow H \rightarrow \gamma\gamma) = \sigma_{SM}(gg \rightarrow H) \cdot BR_{SM}(H \rightarrow \gamma\gamma) \cdot \frac{\kappa_g^2 \cdot \kappa_\gamma^2}{\kappa_H^2}$$

$gg \rightarrow H$ and $H \rightarrow \gamma\gamma$ are loop induced processes at SM $\rightarrow \kappa_g$ and κ_γ are treated as a function of κ_t , κ_b and κ_W .

$\kappa = 1 \rightarrow$ SM expectation

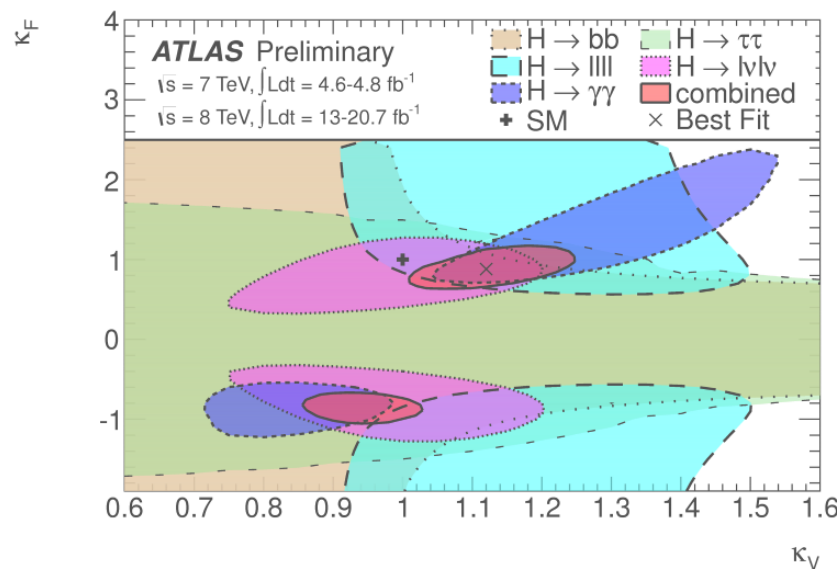
Fermion vs Vector couplings

Different strengths of the fermion and vector couplings are probed:

$$\kappa_V = \kappa_W = \kappa_Z$$

$$\kappa_F = \kappa_t = \kappa_b = \kappa_\tau = \kappa_g$$

Only the relative sign is physical (take $\kappa_V > 0$). Positive relative minimum is preferred but negative relative is compatible within 1σ .



$H \rightarrow \gamma\gamma$ loop depends on κ_F and κ_V . It can be parametrized as:

gg \rightarrow H loop
measures
directly κ_F^2

$$\left| \frac{\kappa_{\gamma\gamma}^2}{\kappa_F^2} \right|^2 \sim \left| \vec{A}_F \times \frac{H}{\kappa_F} \right|^2 + \left| \vec{A}_V \times \frac{H}{\kappa_V} \right|^2$$

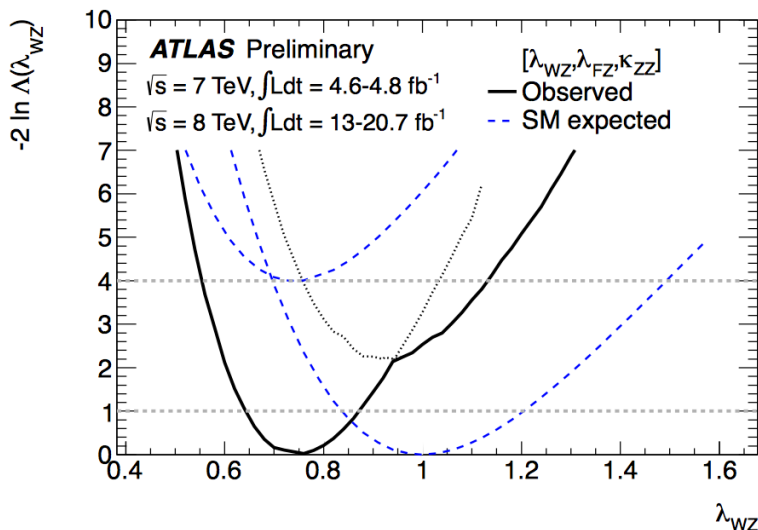
$$\sim 0.07 \kappa_F^2 - 0.66 \kappa_F \kappa_V + 1.59 \kappa_V^2$$

Custodial symmetry

Identical couplings between W- and Z-bosons are required within tight bounds by $SU(2)_L$ custodial symmetry and the ρ parameter at LEP.

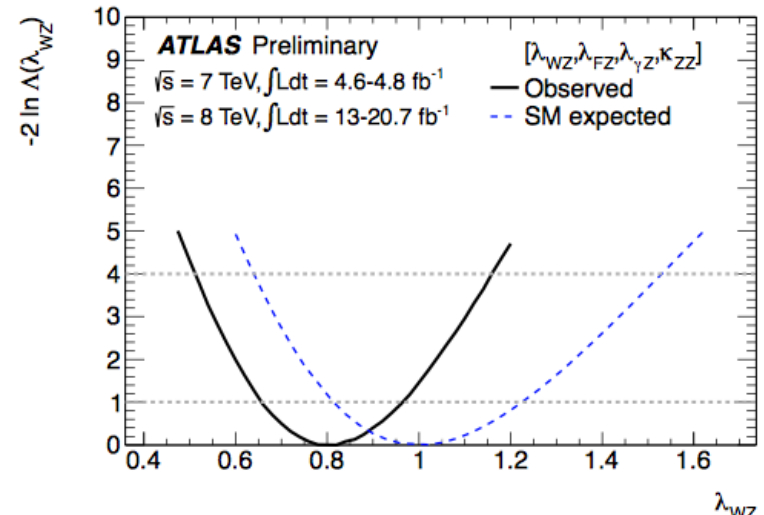
$\lambda_{WZ} = \kappa_W / \kappa_Z$ can be probed in the Higgs sector, while keeping the fermion couplings universal.

$$\begin{aligned}\kappa_{ZZ} &= \kappa_Z \cdot \kappa_Z / \kappa_H \\ \lambda_{WZ} &= \kappa_W / \kappa_Z \\ \lambda_{FZ} &= \kappa_F / \kappa_Z\end{aligned}$$



Assume only SM particles in the $H \rightarrow \gamma\gamma$ loop:

$$\lambda_{WZ} \in [0.64, 0.87]$$



No assumption on the $H \rightarrow \gamma\gamma$ loop:

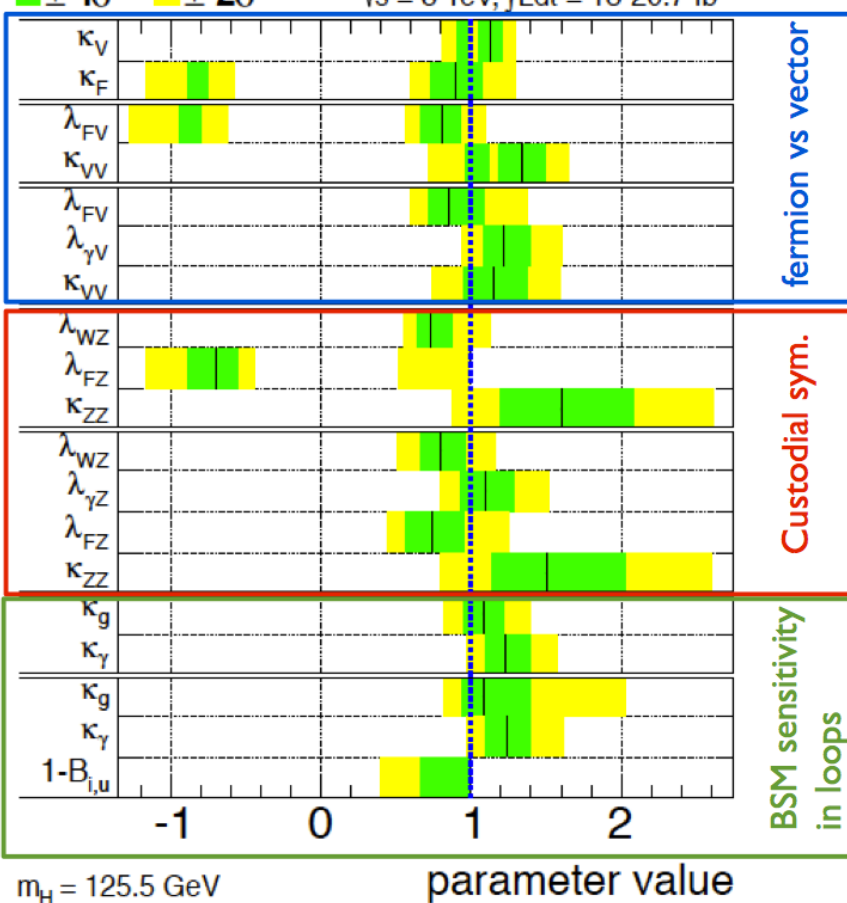
$$\lambda_{WZ} = 0.80 \pm 0.15$$

Couplings summary

ATLAS Preliminary

$\sqrt{s} = 7 \text{ TeV}, \int L dt = 4.6\text{-}4.8 \text{ fb}^{-1}$

$\sqrt{s} = 8 \text{ TeV}, \int L dt = 13\text{-}20.7 \text{ fb}^{-1}$



→ SM

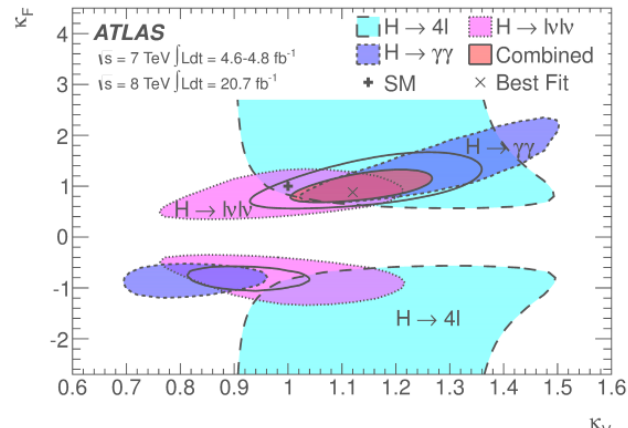
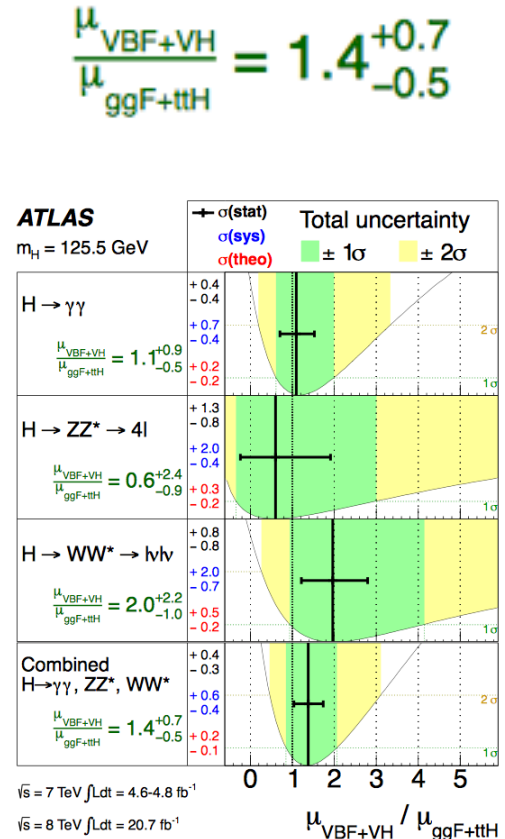
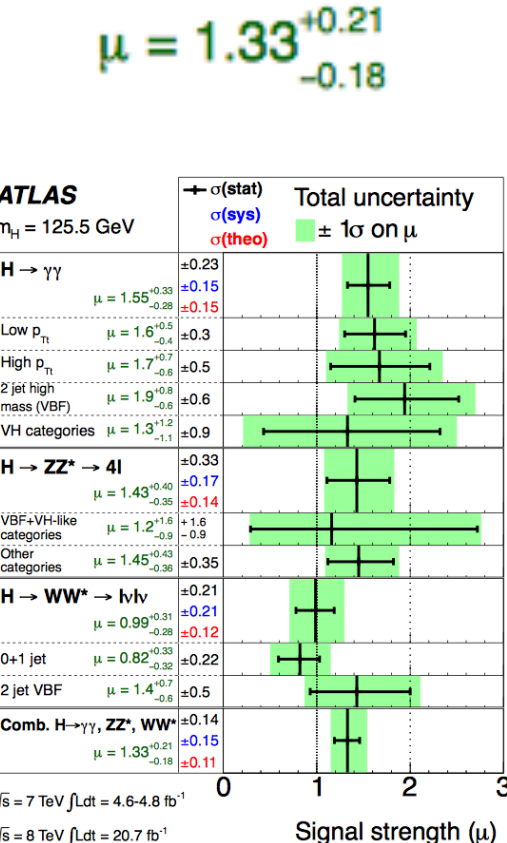
→ Free total width

→ Free $H \rightarrow \gamma\gamma$ loop content

→ SM

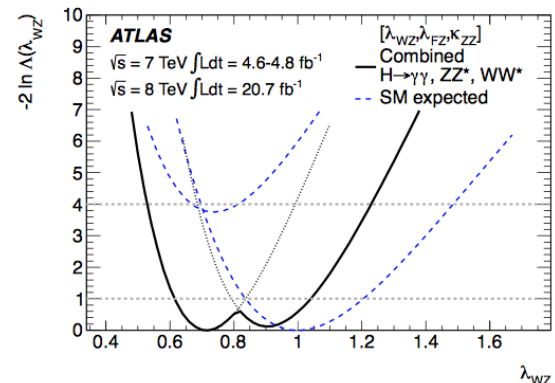
→ Free $H \rightarrow \gamma\gamma$ loop content

$\gamma\gamma$, ZZ^* , WW^* - combination



$$K_F \in [0.76, 1.18]$$

$$K_V \in [1.05, 1.22]$$



$$\lambda_{WZ} = 0.82 \pm 0.15$$

Summary

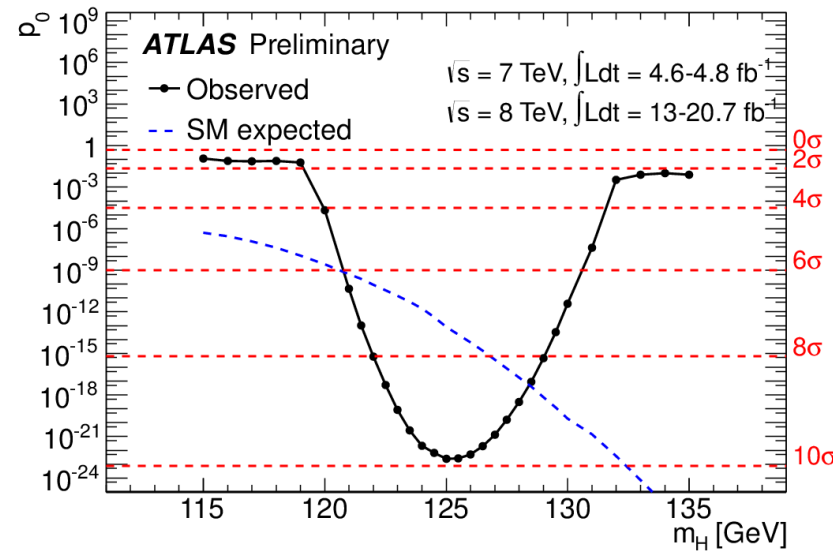
Summary

ATLAS has discovered a new particle, a Higgs boson.
The significance of this discovery reached 10σ with 25fb^{-1} (full Run I data) for $H \rightarrow \gamma\gamma$, $H \rightarrow ZZ$ and $H \rightarrow WW$ decay channels, and 18fb^{-1} for $H \rightarrow bb$ and $H \rightarrow \tau\tau$.

Since the discovery, the focus has shifted on measuring the properties of this Higgs boson.

Executive summary:

- mass - $125.5 \pm 0.2 \text{ (stat)}^{+0.5}_{-0.6} \text{ (sys) GeV}$
- spin-parity $J^P - 0^+$
- couplings in agreement with the SM expectation



Optimized analyses from for $H \rightarrow \gamma\gamma$, $H \rightarrow ZZ$ and $H \rightarrow WW$ will soon become public → followed by the final Run I Higgs combination!

Backup

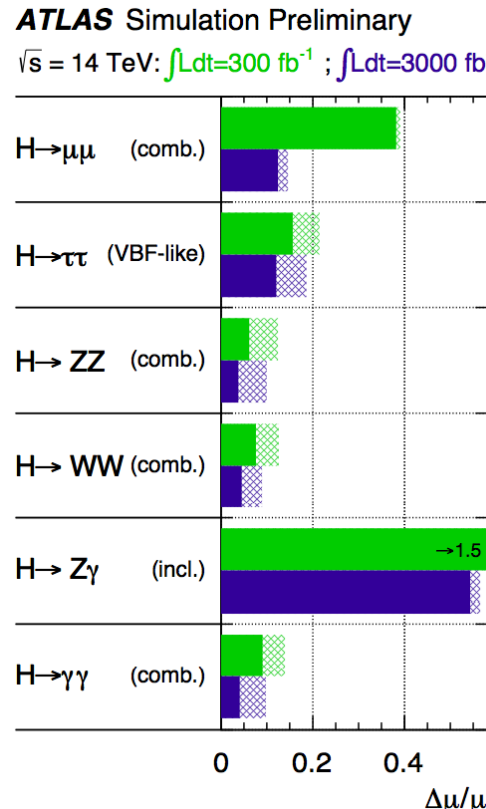
Projections of the uncertainties on the global signal strength

Studies on measuring the properties of the Higgs boson have been performed assuming:

- 14 TeV p-p collisions with 300fb^{-1} , PU-50-60
- 14 TeV p-p collisions at the HL-LHC with 3ab^{-1} , PU-140

Assumptions made:

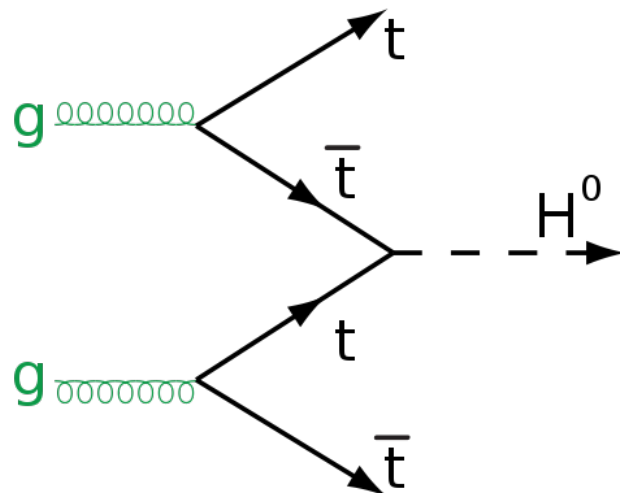
- Performance in high pileup conditions
- Reduction in the experimental and theoretical uncertainties



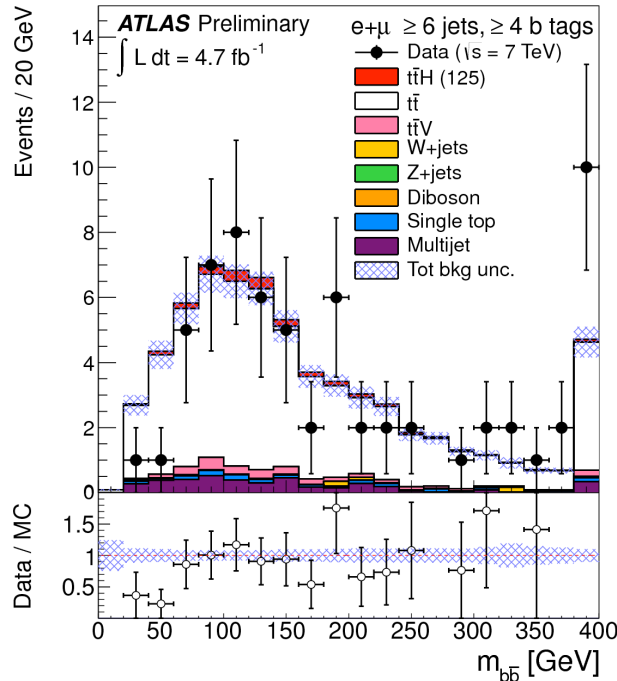
Higgs Boson Decay	μ ($m_H = 125.5 \text{ GeV}$)
$VH \rightarrow Vbb$	-0.4 ± 1.0
$H \rightarrow \tau\tau$	0.8 ± 0.7
$H \rightarrow WW^{(*)}$	1.0 ± 0.3
$H \rightarrow \gamma\gamma$	1.6 ± 0.3
$H \rightarrow ZZ^{(*)}$	1.5 ± 0.4
Combined	1.30 ± 0.20

Current (Run I data) signal strength uncertainties.

- Very challenging search
 - ◆ Small cross-section, large backgrounds
 - ◆ Large theoretical uncertainties
- The only way to measure directly the top Yukawa coupling
- Analyses statistically limited with current LHC dataset
- ATLAS has explored the $b\bar{b}$ and $\gamma\gamma$ Higgs boson decays

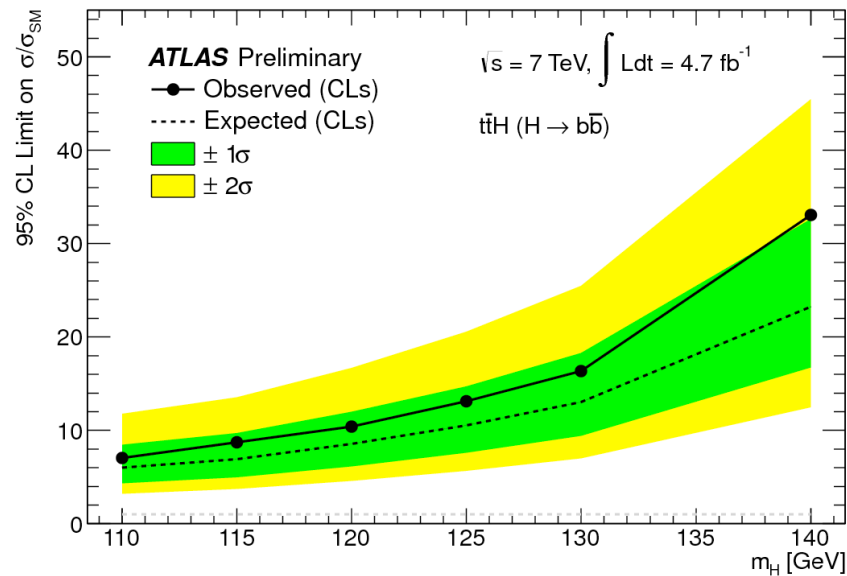


ttH(bb)

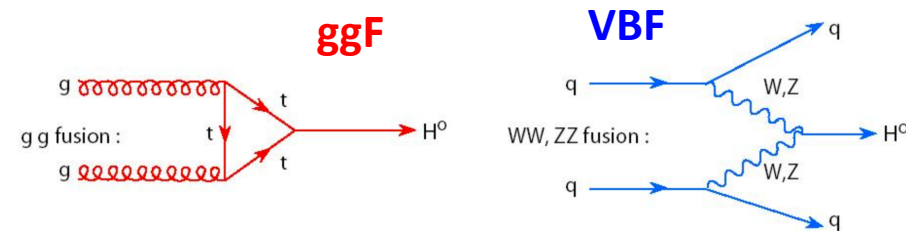
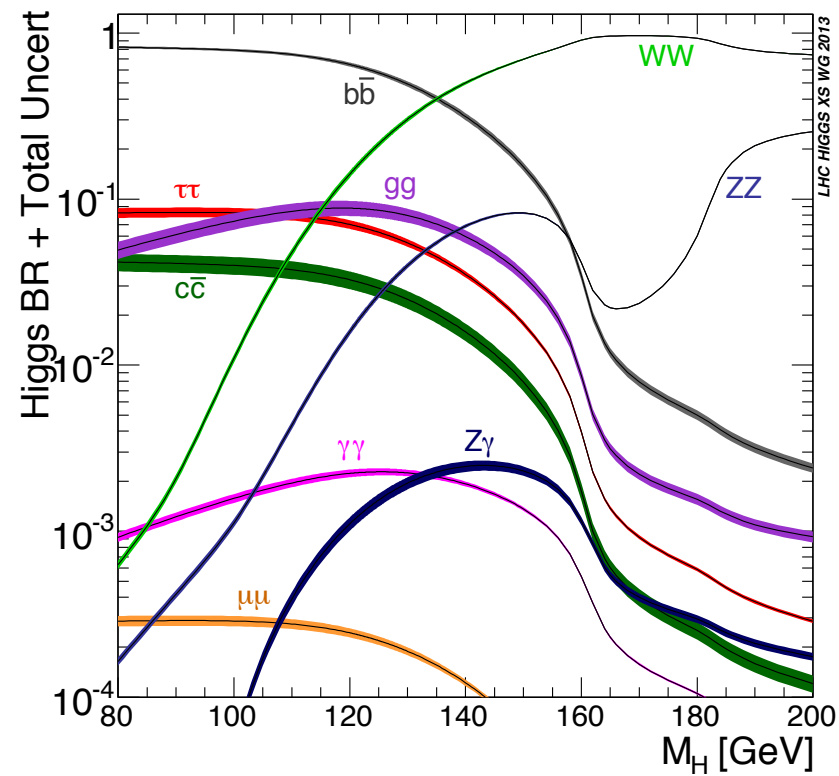
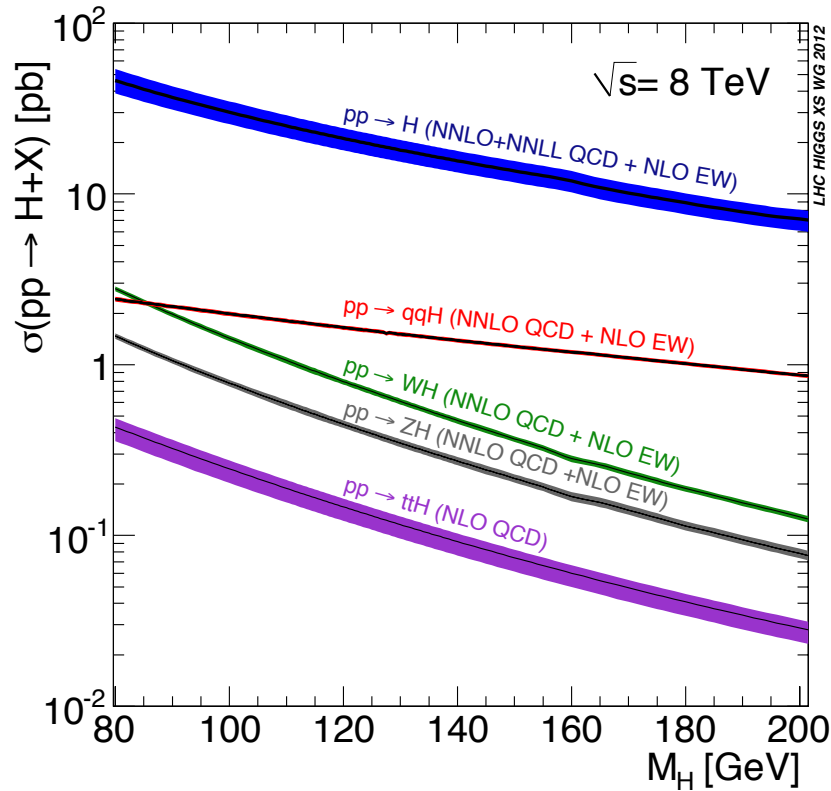


- 7 TeV only
- Semi-leptonic top decays
- N_{jet} and $N_{\text{b-tagged jets}}$ categories to reduce backgrounds and constrain systematic uncertainties
 - ◆ Most powerful category: 4 b-tagged + 2 additional jets
- Main challenges: ttbar background modelling
- Discriminating variables m_{bb} , H_T

- Leading uncertainties
 - ◆ Jet energy scale, b-tagging efficiency, theory
- 95% CL Limits:
observed(expected)
 $13(10.5) \times \text{SM}$ for $m_H = 125 \text{ GeV}$

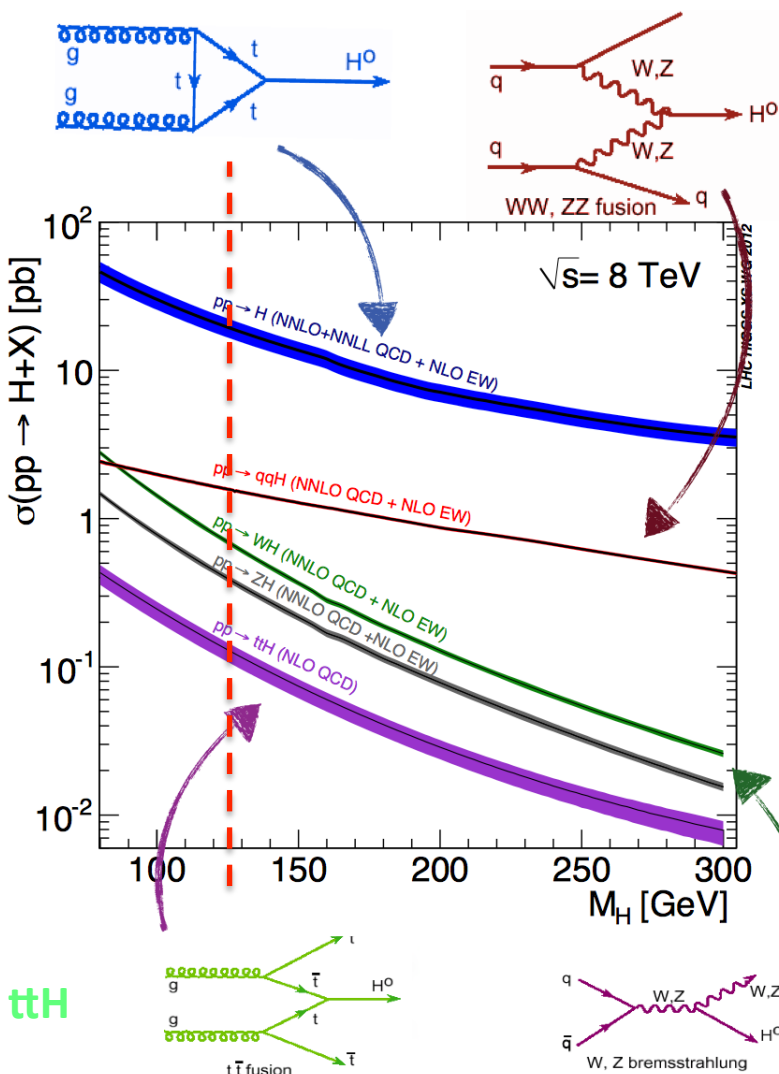


Production and decay modes

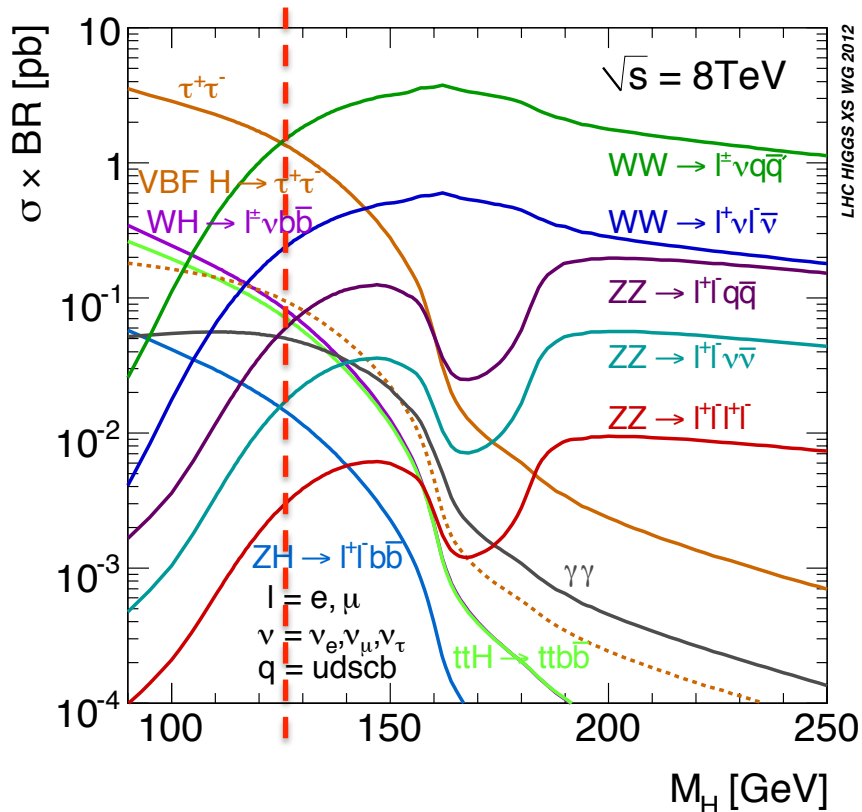


Production and decay modes

ggF



VBF



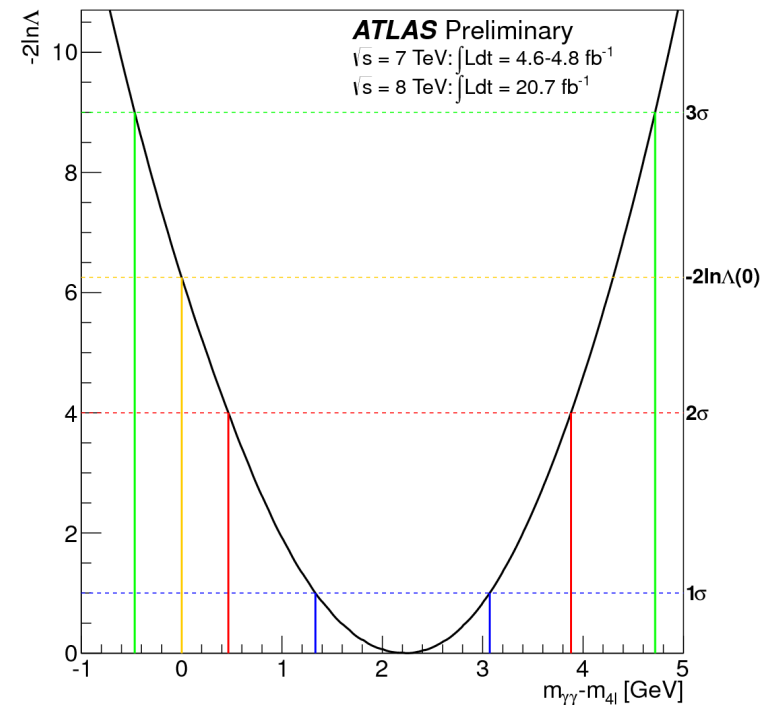
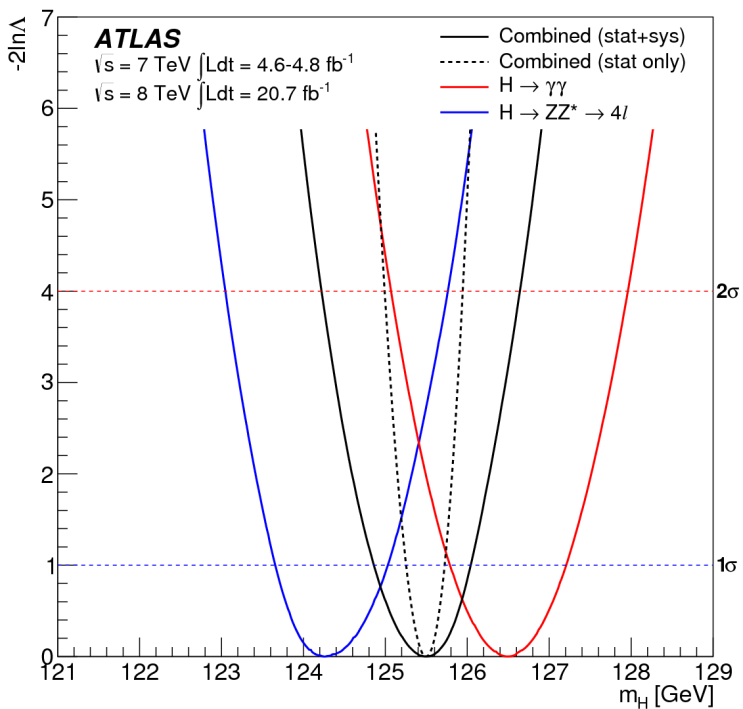
WH/ZH

Mass

Higgs boson's mass is extracted from the mass measurements from two channels:

$$\begin{aligned} H \rightarrow \gamma\gamma & \quad 126.8 \pm 0.2 \text{ (stat)} \pm 0.7 \text{ (sys)} \text{ GeV} \\ H \rightarrow ZZ^* \rightarrow 4l & \quad 124.3^{+0.6}_{-0.5} \text{ (stat)}^{+0.5}_{-0.3} \text{ (sys)} \text{ GeV} \end{aligned}$$

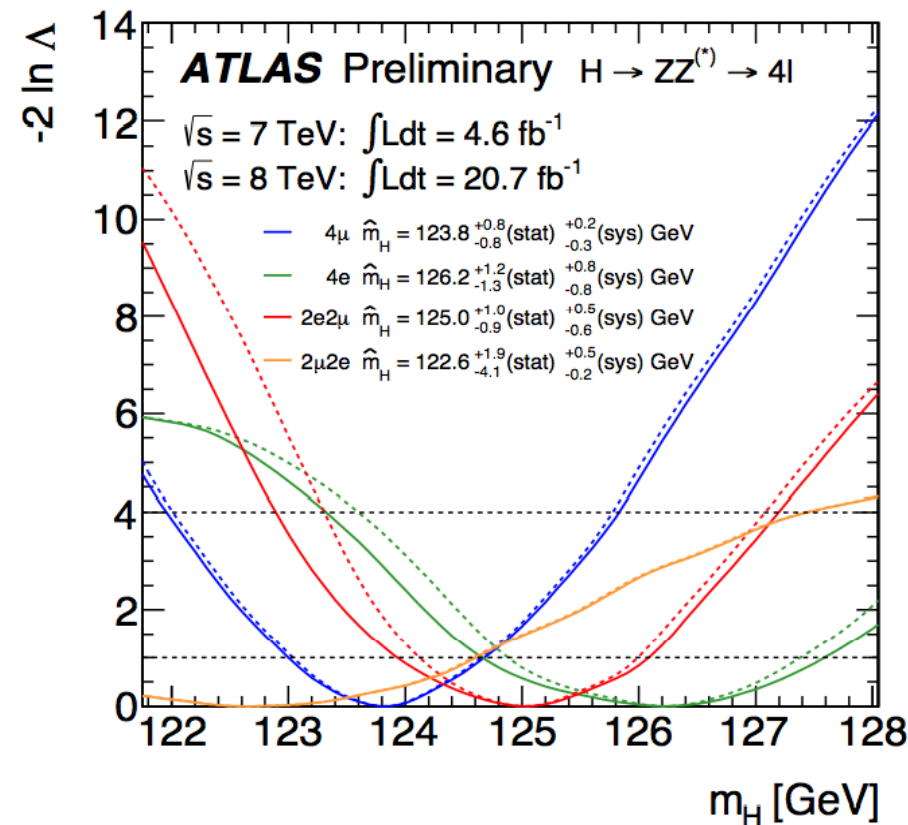
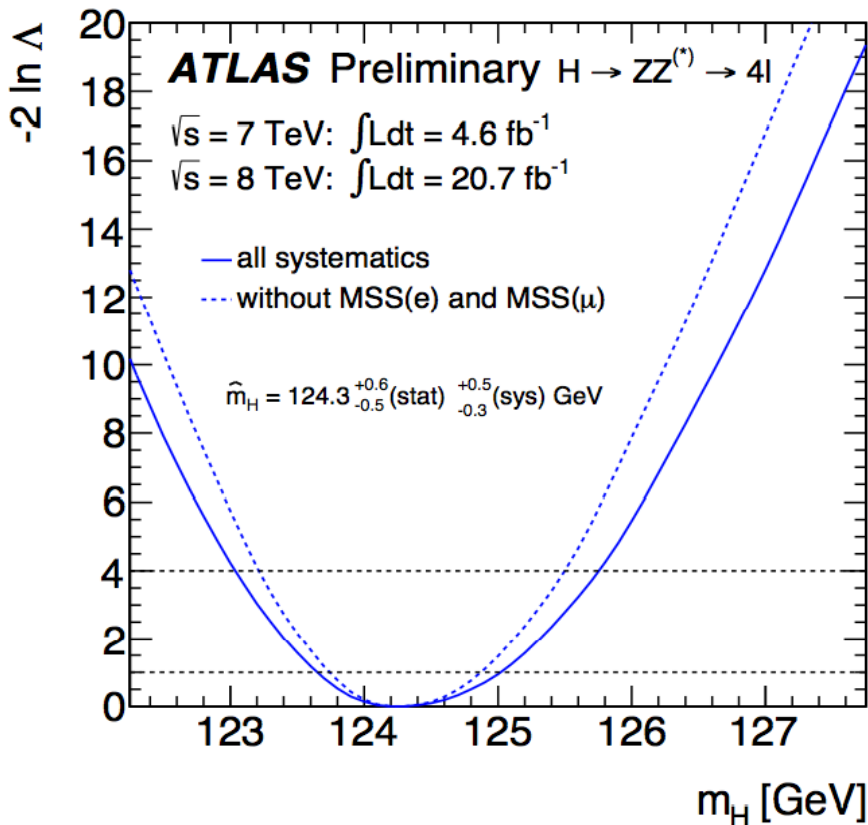
$$m_H = 125.5 \pm 0.2 \text{ (stat)}^{+0.5}_{-0.6} \text{ (sys)} \text{ GeV}$$



Profile likelihood ratio scan $-2\ln\Lambda(\alpha)$, with a parameter of interest α :

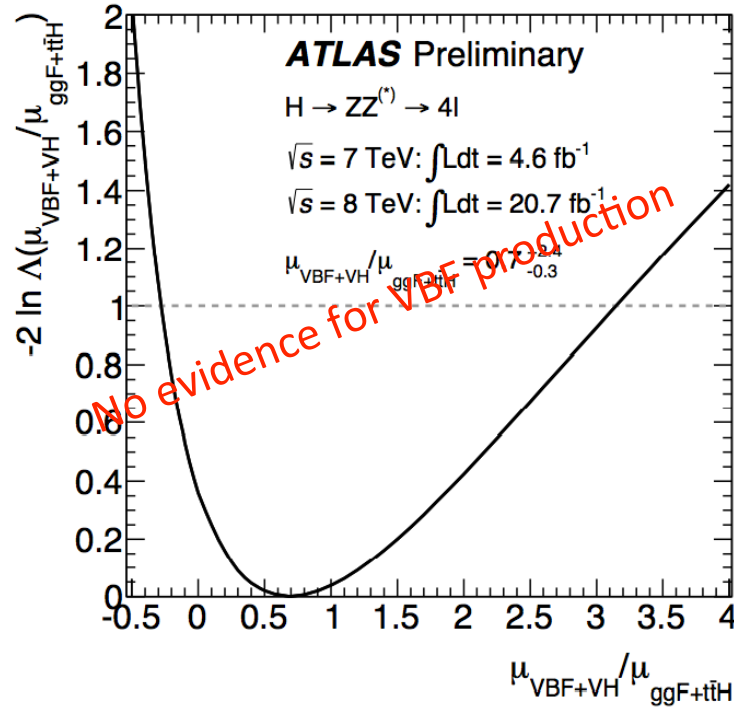
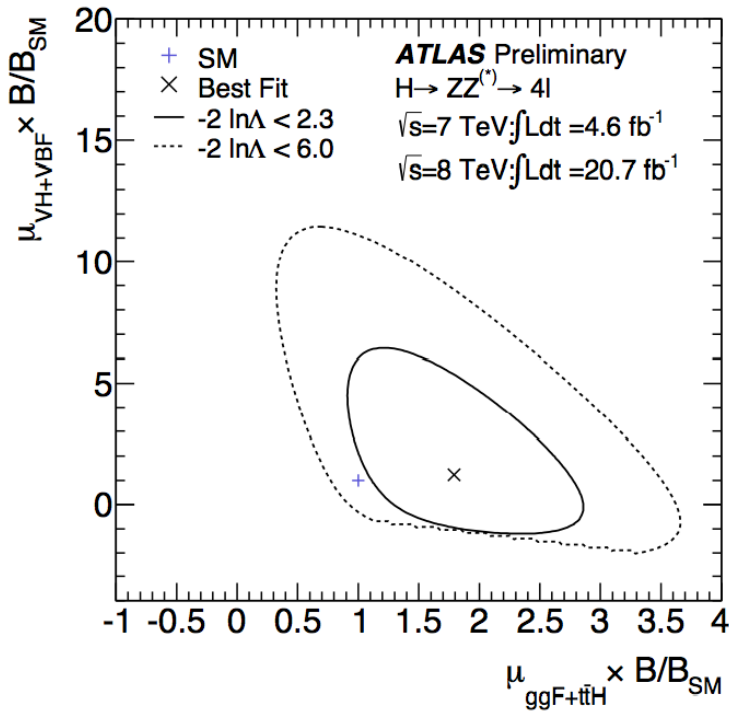
- $-2\ln\Lambda(\alpha)=0$ – provides a best-fit value of α
- $-2\ln\Lambda(\alpha)=1$ – provides a 1σ interval around the best-fit value of α
- $-2\ln\Lambda(0)$ – provides a compatibility of the best-fit value α , with $\alpha = 0$

$H \rightarrow ZZ^* \rightarrow 4l$ mass



Systematics dominated by the energy and momentum scale uncertainties.

$H \rightarrow ZZ^* \rightarrow 4l$ couplings



B/B_{SM} is included since in the single channel analysis, the source of potential new physics cannot be resolved between production and decay.

The cut-off is there for $S+B=0 \rightarrow$ golden channel with high S/B ratio.

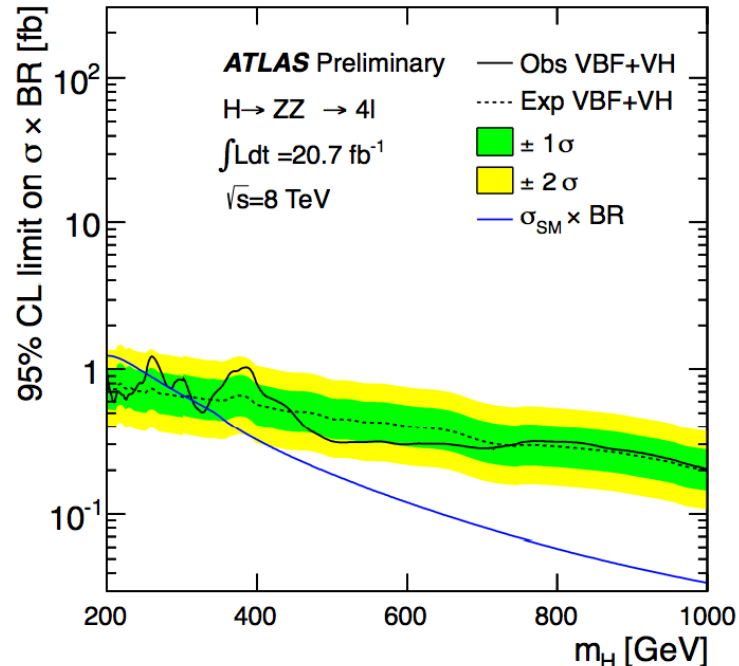
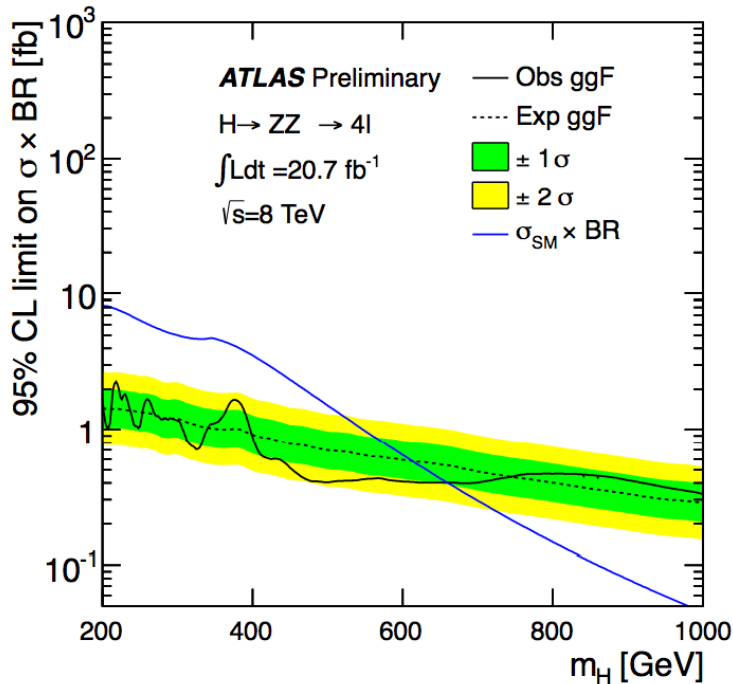
2/27/14

$\mu_{ggF+t\bar{t}H} \times B/B_{SM}$ and $\mu_{VBF+VH} \times B/B_{SM}$

$1.8^{+0.8}_{-0.5}$ and $1.2^{+3.8}_{-1.4}$

$\mu_{VBF+VH}/\mu_{ggF+t\bar{t}H}$ $0.7^{+2.4}_{-0.3}$

$H \rightarrow ZZ^* \rightarrow 4l$ high mass



95% upper limits on the production times the BR. Heavy Higgs boson line-shape – CPS is used. Expected SM Higgs boson x-sec times BR is shown as well.

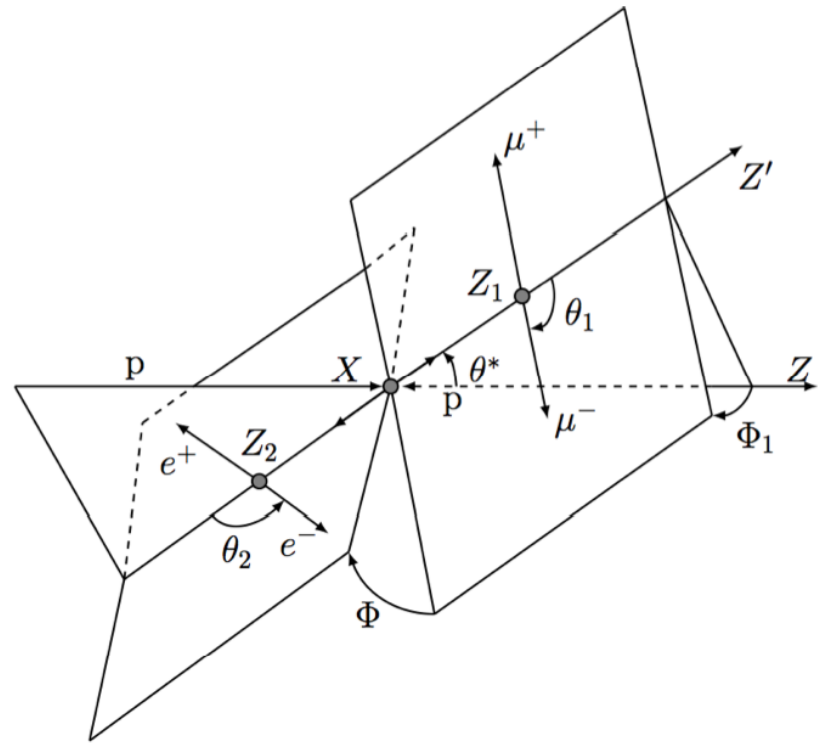
No sensitivity to the VBF production!

$H \rightarrow ZZ^* \rightarrow 4l$

spin-parity

Variables sensitive to the spin and parity of the Higgs boson:

- the masses of two Z bosons,
- the production angle θ^* of Z_1 defined in the four lepton rest frame,
- and 4 decay angles:

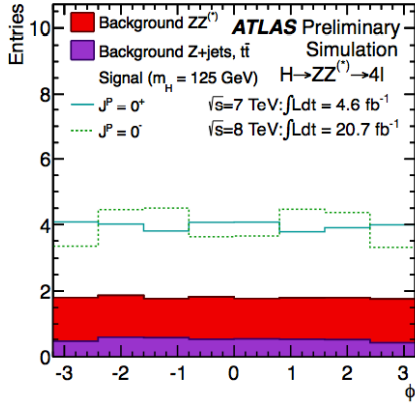


- θ_1 (θ_2) is the angle between the negative final state lepton and the direction of flight of Z_1 (Z_2) in the Z rest frame.
- Φ is the angle between the decay planes of the four final state leptons expressed in the four lepton rest frame.
- Φ_1 is the angle defined between the decay plane of the leading lepton pair and a plane defined by the vector of the Z_1 in the four lepton rest frame and the direction of the parton following the positive z axis.

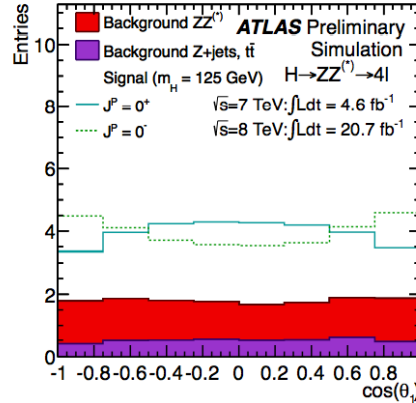
$H \rightarrow ZZ^* \rightarrow 4l$

spin-parity

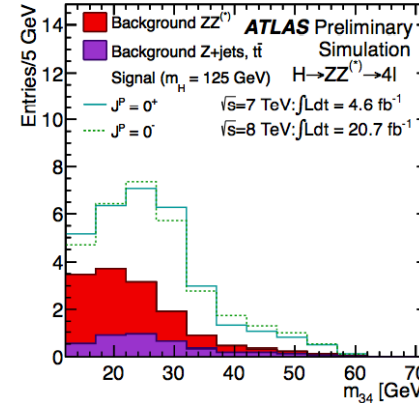
0+, 0-, 1+,1-, 2+m, 2-
 2+m analyzed in 25% steps of fqq
 115-130 GeV only – split into 3 categories with
 varying S/B ratio (6% increase in sensitivity with
 this split)



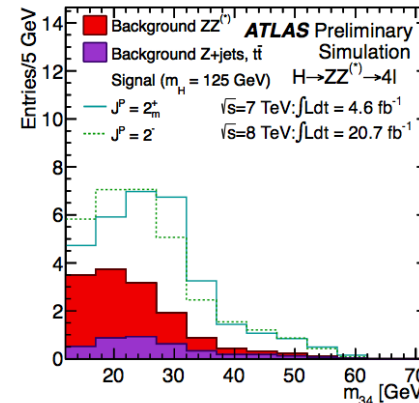
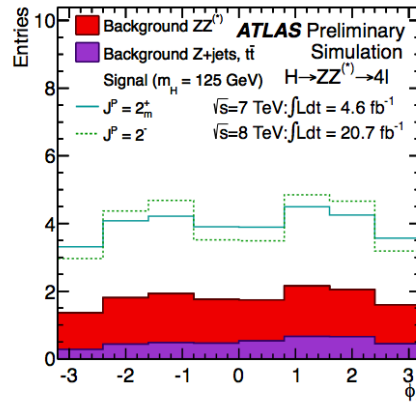
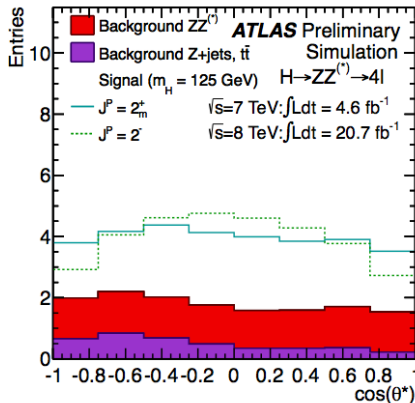
(a)



(b)



(c)



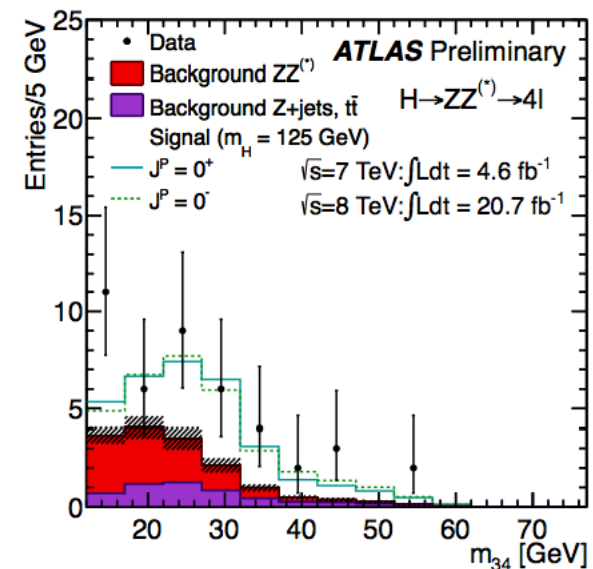
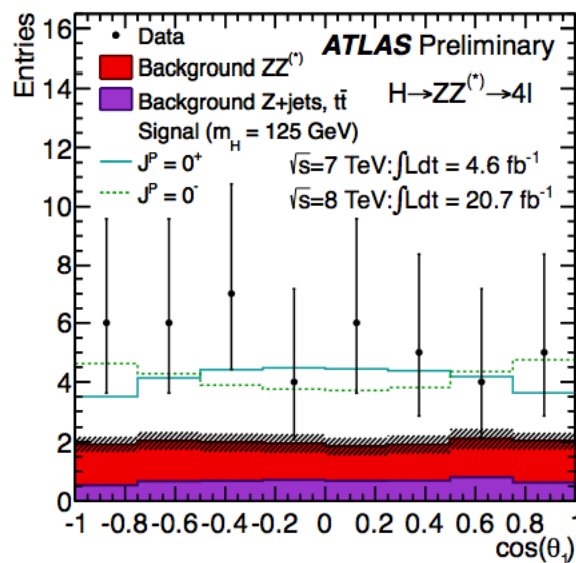
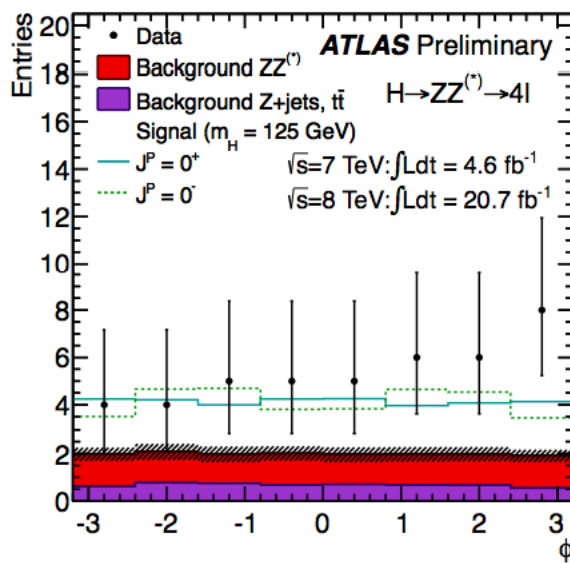
$H \rightarrow ZZ^* \rightarrow 4l$ spin-parity

$$\mathcal{P}^{ij} = \mu^{\text{sig}} f_i^{\text{sig}} N_{\text{sig}} \left[(1 - \varepsilon) \cdot \text{PDF}_{H_0}^{ij} + \varepsilon \cdot \text{PDF}_{H_1}^{ij} \right] \\ + \sum_{\text{bkg}_k} f_i^{\text{bkg}_k} N_{\text{bkg}_k} \text{PDF}_{\text{bkg}_k}^{ij},$$

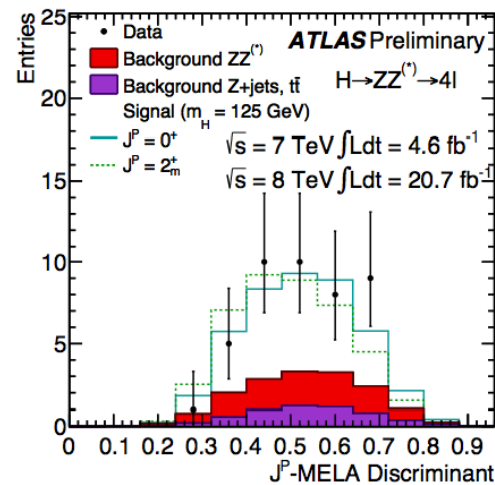
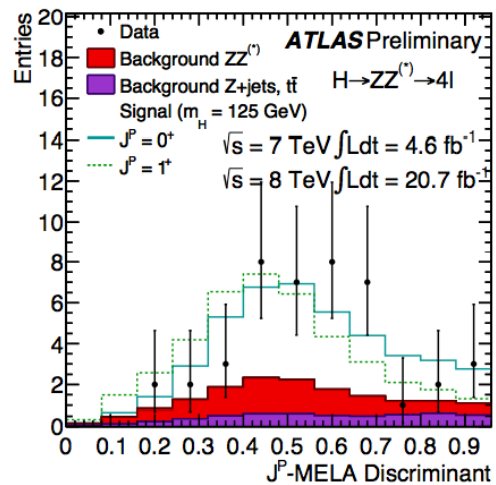
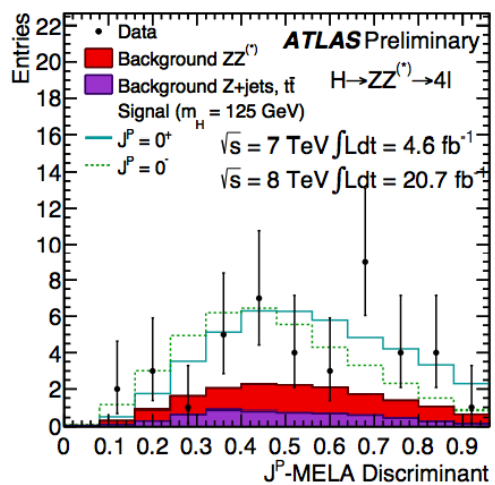
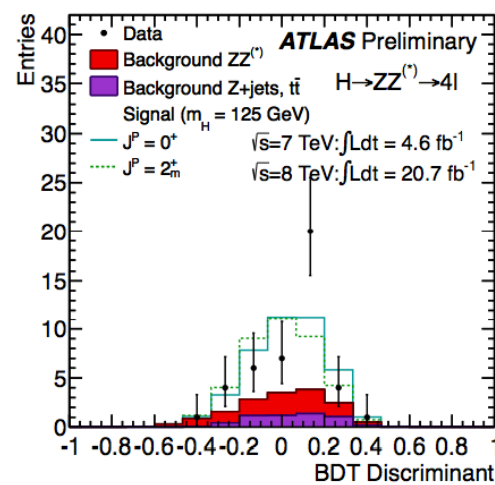
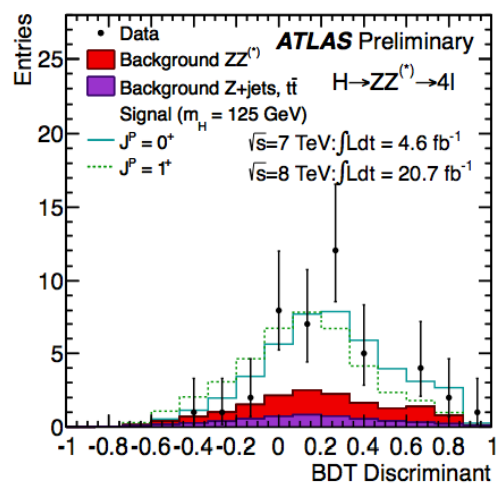
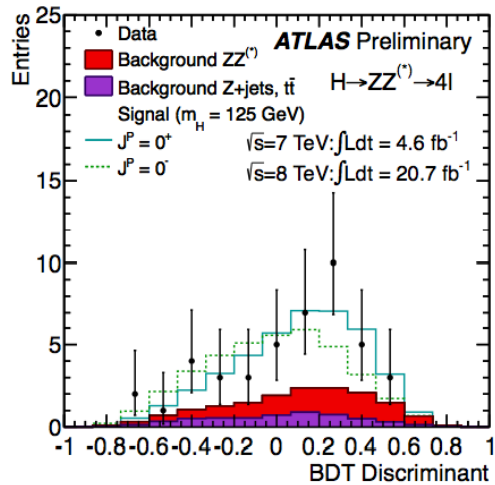
Two methods:

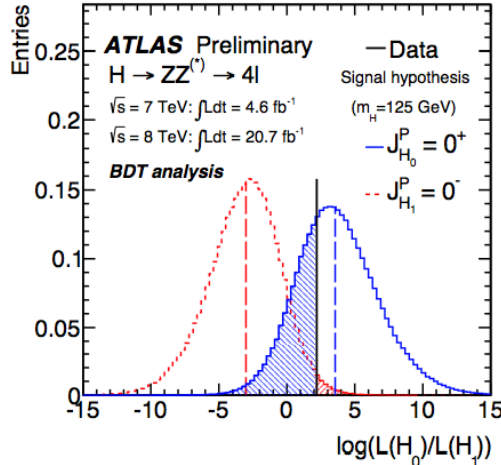
- BDT – trained for each spin-parity state, BDT response is added to the profile likelihood ratio fit
- MELA – matrix-element likelihood ratio analysis (theoretical differential decay rate (angles and masses) corrected for detector acceptance and analysis selection) – PDF discriminant

$$\log[L(H_1)/L(H_0)],$$

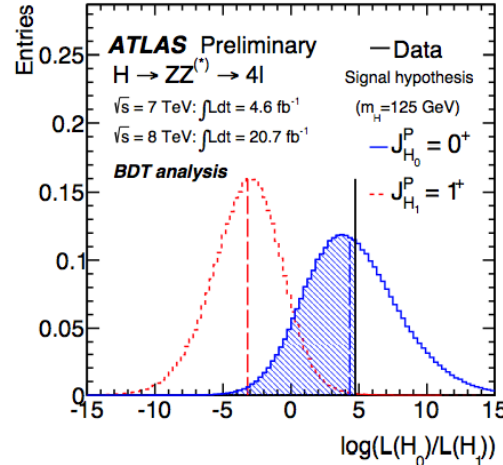


100% ggF for 2+m hypothesis

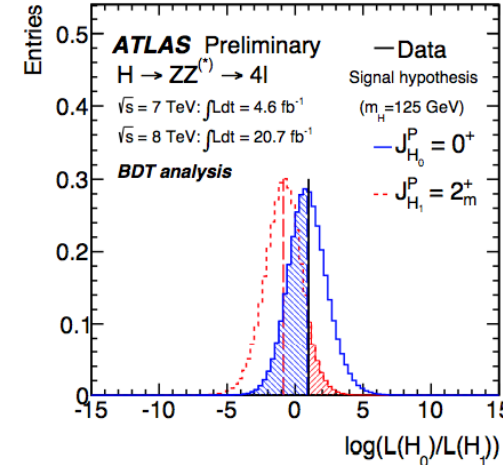




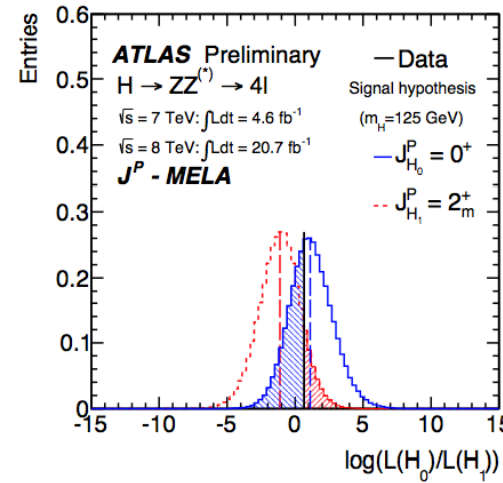
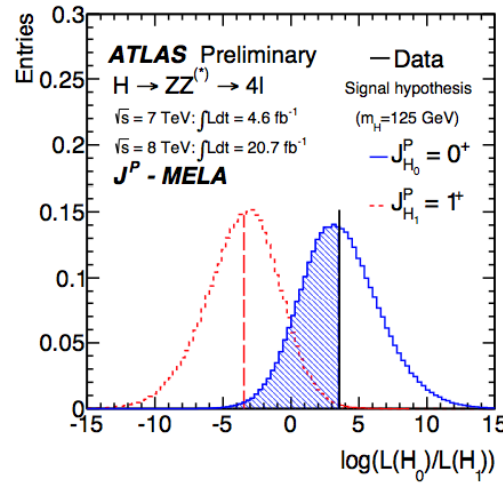
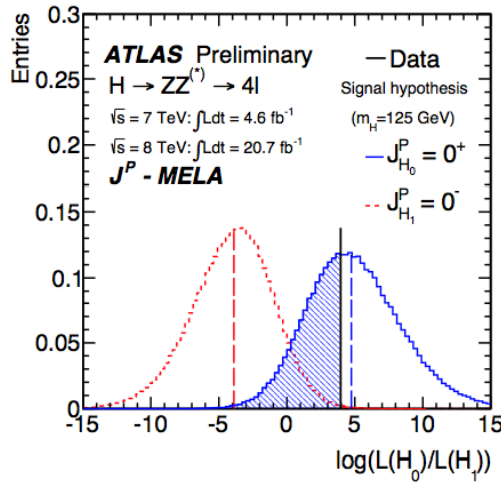
(a)



(b)

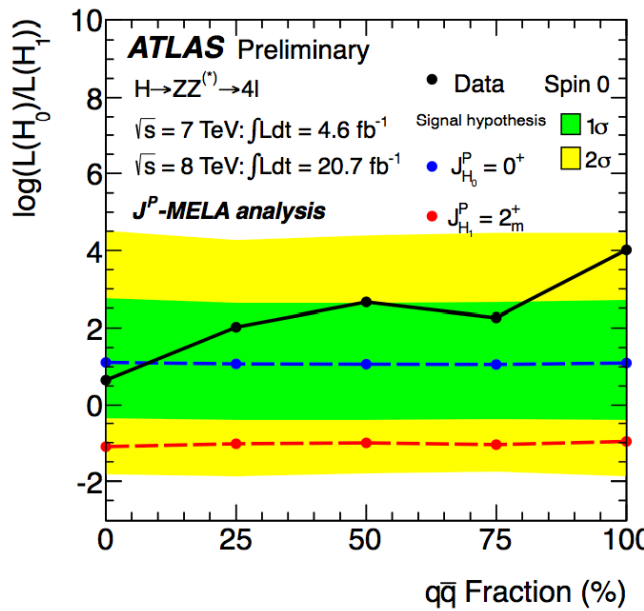
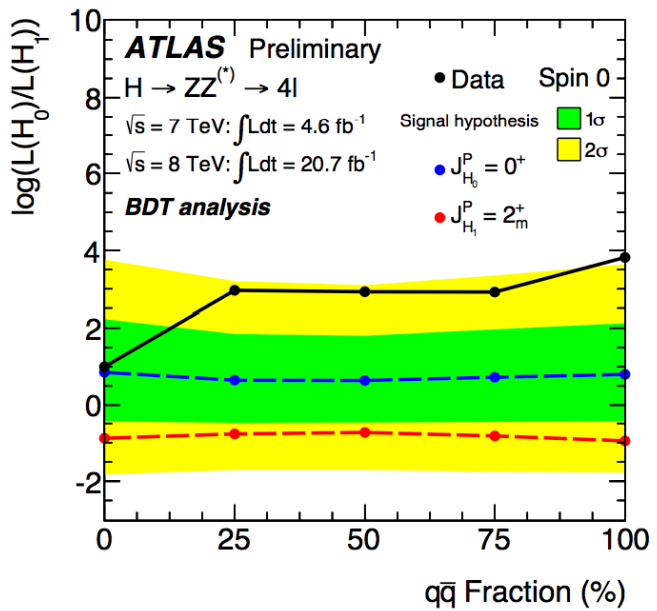


(c)



Shaded areas correspond to the observed p_0 -values for H_0 and H_1 hypotheses.

100% ggF for 2+m hypothesis



$$CL_S = p_0(\text{alternative } J^P) / (1 - p_0(0^+)).$$

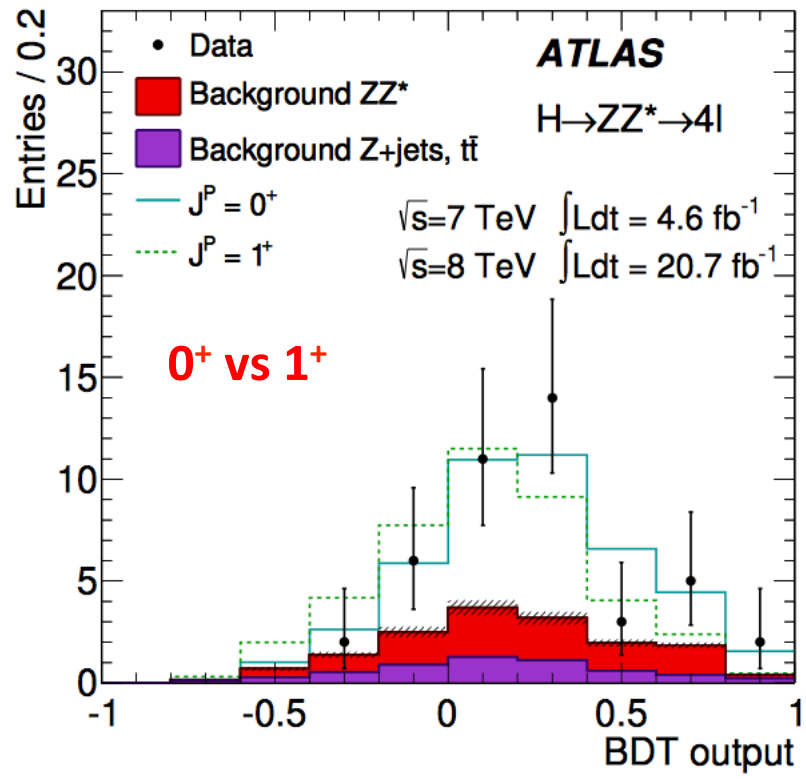
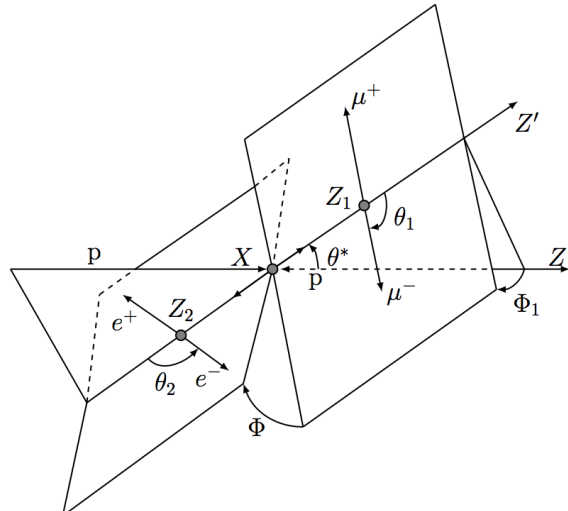
		BDT analysis			CL _S	J^P -MELA analysis			
		tested J^P for an assumed 0^+		tested 0^+ for an assumed J^P		tested J^P for an assumed 0^+		tested 0^+ for an assumed J^P	
		expected	observed	observed*		expected	observed	observed*	
0 ⁻	p_0	0.0037	0.015	0.31	0.022	0.0011	0.0022	0.40	0.004
1 ⁺	p_0	0.0016	0.001	0.55	0.002	0.0031	0.0028	0.51	0.006
1 ⁻	p_0	0.0038	0.051	0.15	0.060	0.0010	0.027	0.11	0.031
2 ⁺ _m	p_0	0.092	0.079	0.53	0.168	0.064	0.11	0.38	0.182
2 ⁻	p_0	0.0053	0.25	0.034	0.258	0.0032	0.11	0.08	0.116

Spin-Parity

SM spin-parity $J^P = 0^+$ hypothesis is compared with alternatives from three channels:
 $H \rightarrow \gamma\gamma$, $H \rightarrow ZZ^*$ and $H \rightarrow WW^*$

Hypotheses tested are: 0^- , 1^+ , 1^- and 2^+ .

$H \rightarrow ZZ^*$ – reconstructed masses of two Z bosons, 1 production and 4 decay angles, serve as inputs to BDT

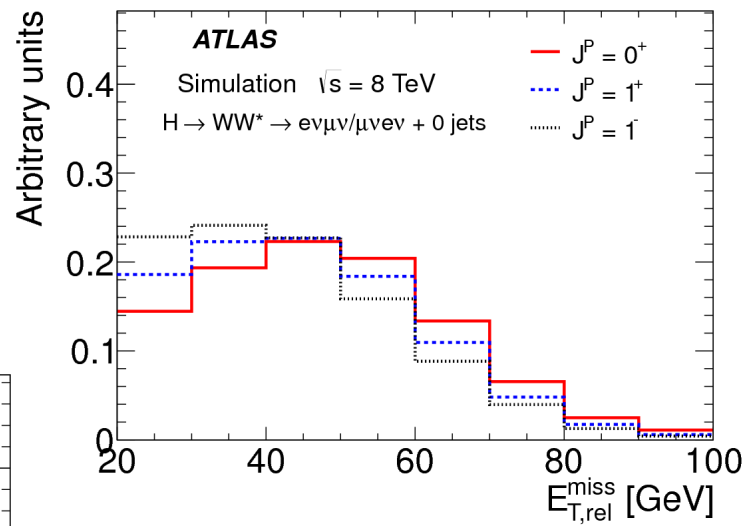
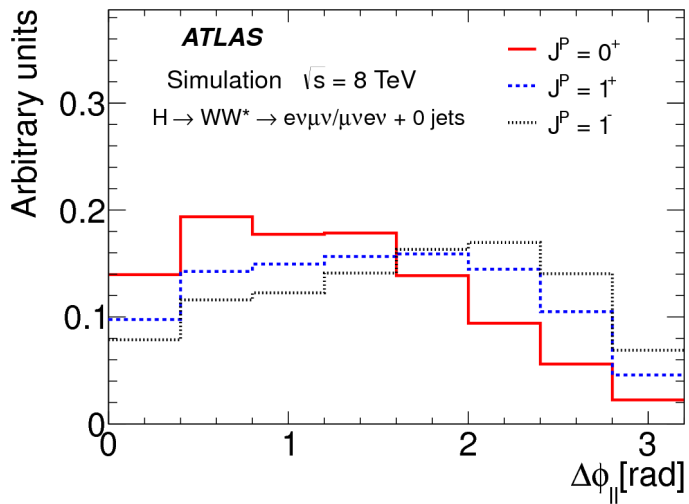


Spin-Parity

SM spin-parity $J^P = 0^+$ hypothesis is compared with alternatives from three channels:
 $H \rightarrow \gamma\gamma$, $H \rightarrow ZZ^*$ and $H \rightarrow WW^*$

Hypotheses tested are: 0^- , 1^+ , 1^- and 2^+ .

$H \rightarrow WW^*$ – $\Delta\Phi(\text{ll})$, $m(\text{ll})$, $pT(\text{ll})$
 and m_T
 serve as inputs to BDT.



Cuts used in the couplings analysis have to be loosened to increase the sensitivity to alternative J^P hypotheses.

Spin-parity combination

$$\mathcal{L}(J^P, \mu, \theta) = \prod_j^{N_{\text{chann.}}} \prod_i^{N_{\text{bins}}} P(N_{i,j} | \mu_j \cdot S_{i,j}^{(J^P)}(\theta) + B_{i,j}(\theta)) \times \mathcal{A}_j(\theta),$$

$$q = \log \frac{\mathcal{L}(J^P = 0^+, \hat{\mu}_{0^+}, \hat{\theta}_{0^+})}{\mathcal{L}(J_{\text{alt}}^P, \hat{\mu}_{J_{\text{alt}}^P}, \hat{\theta}_{J_{\text{alt}}^P})}$$

Test statistic q is used to determine the p₀-values. Expected are derived using ensemble tests (MC pseudo-experiments).

MLE evaluated under different spin-parity hypotheses

A product of Poisson distributions P corresponding to the observation of Nij events given Sij and Bij. Nuisance parameters, θ , are constrained by auxiliary measurements.

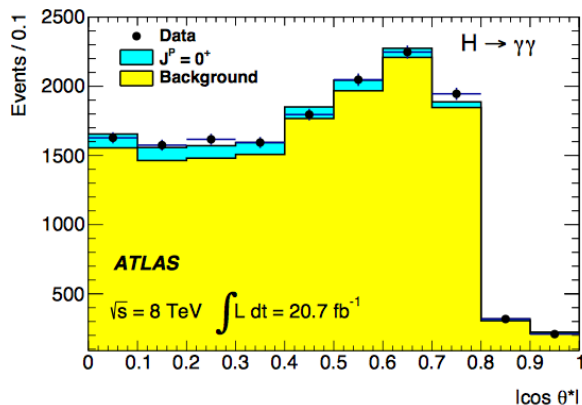
Couplings to the Higgs boson with the alternative hypotheses are not known – treated as nuisance parameters in the fit.

Expected p0-value is obtained after integrating the test-statistic distribution above the median for the tested hypothesis.
If the observed agrees with the tested hypothesis then the observed p0 will be 50%.

$H \rightarrow \gamma\gamma$ spin-parity

The selection is the same as the couplings analysis with an important requirement that the transverse momenta of the photons are proportional to the invariant mass of the photons → reduces the correlation between $m_{\gamma\gamma}$ and $|\cos\theta^*|$ for the background to a negligible level. $105 < m_{\gamma\gamma} < 160$ GeV mass is chosen, 122-130 is treated as the signal region, the rest is the side-bands.

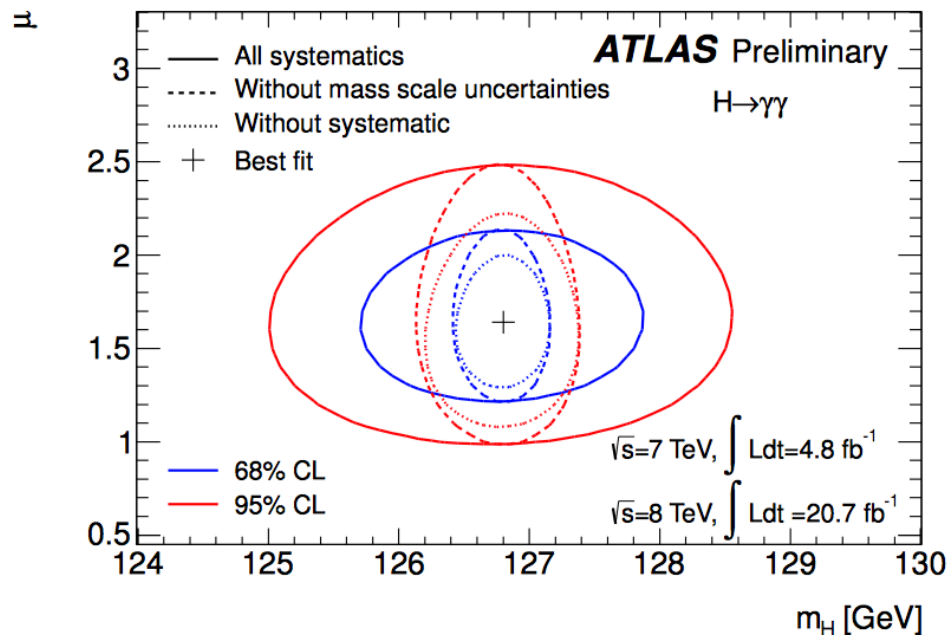
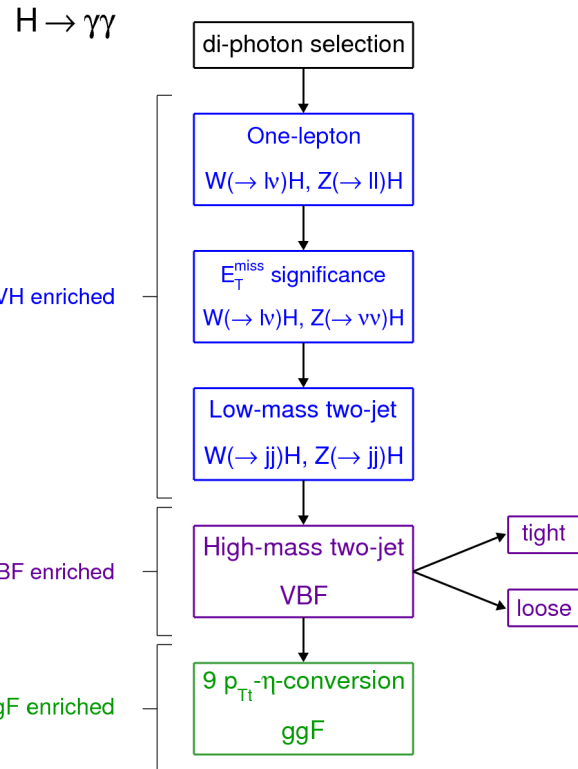
Signal in bins of $|\cos\theta^*|$ is corrected for the interference with $gg \rightarrow \gamma\gamma$ for spin-0 hypothesis → the correction value is taken as systematics



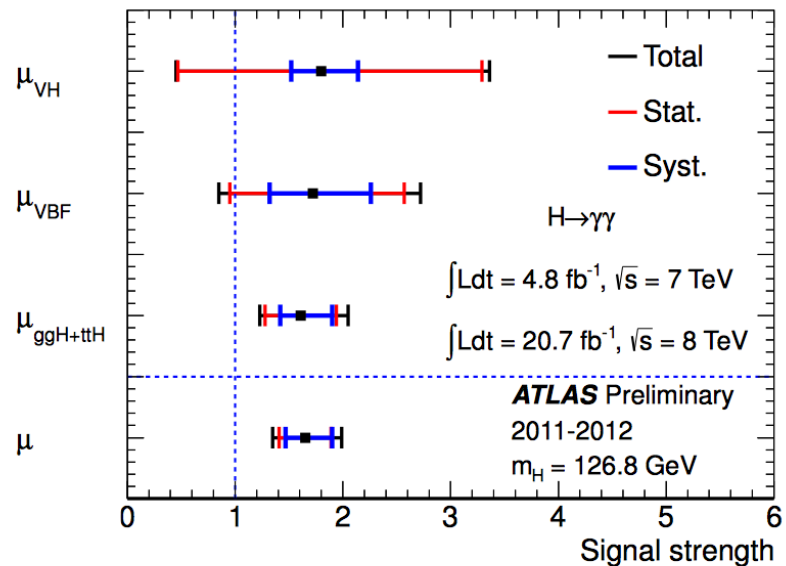
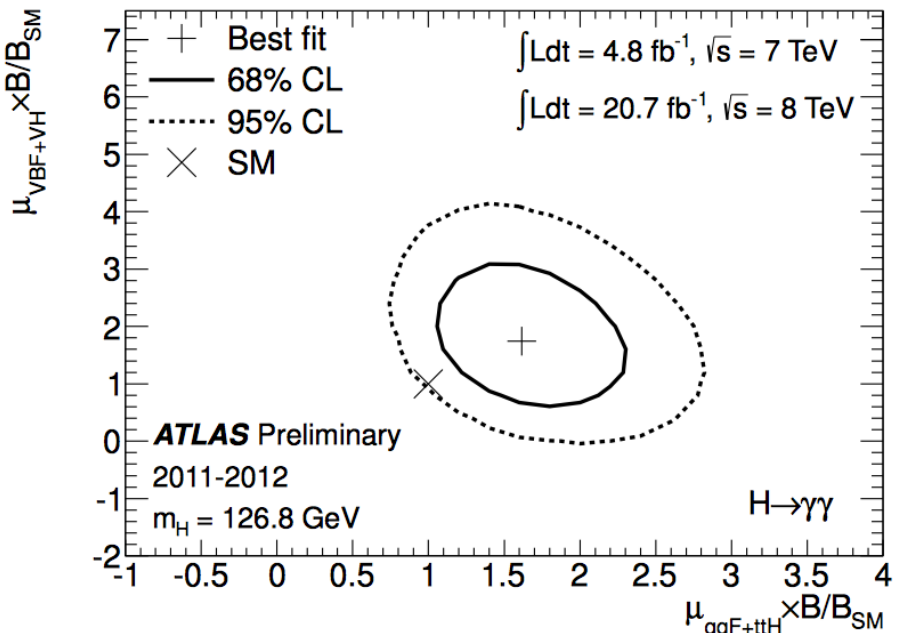
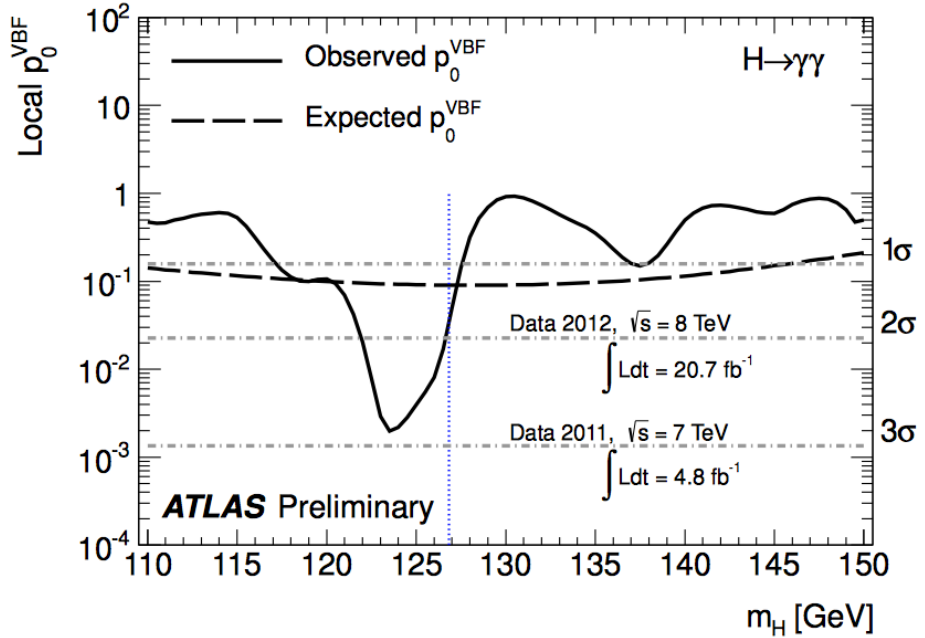
In the background-subtracted plots, the data points differ a bit, because the fitted background depends on the profiling of the nuisance parameters associated with the bin-by-bin systematics.

$H \rightarrow \gamma\gamma$

ATLAS Preliminary



Mass scale – photon energy scale uncertainties



Fermion vs Vector coupling

Different strengths of the fermion and vector couplings are probed (only SM particles in the $gg \rightarrow H$ and $H \rightarrow \gamma\gamma$ loops, and SM Higgs boson decays modes entering the total width):

$$\kappa_V = \kappa_W = \kappa_Z$$

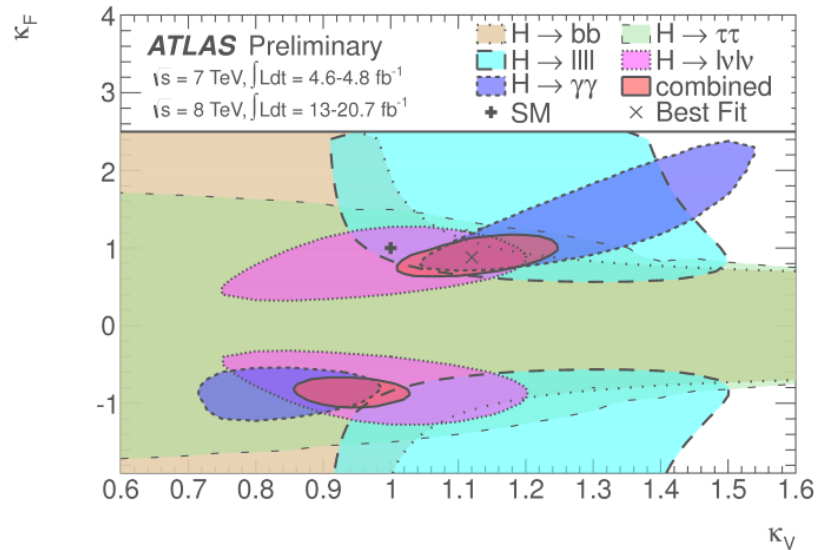
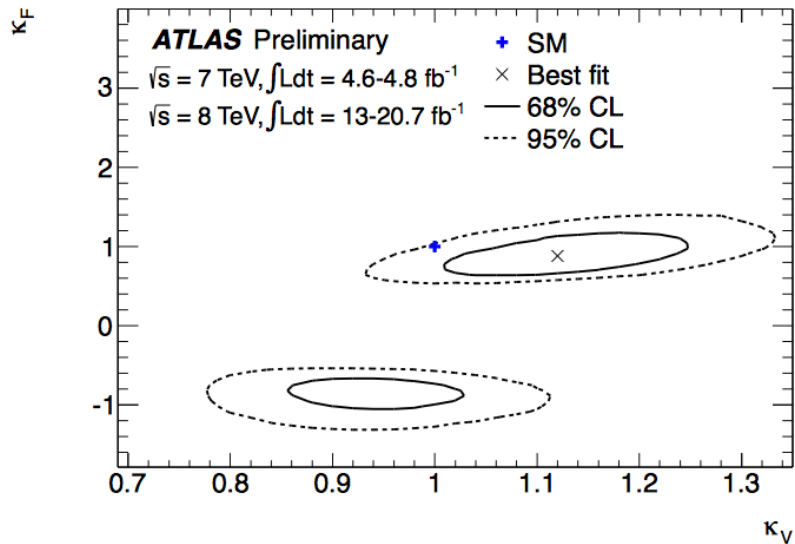
$$\kappa_F = \kappa_t = \kappa_b = \kappa_\tau = \kappa_g$$

Assume only SM particles allowed in $gg \rightarrow H \rightarrow$ measure directly κ_F^2 ;
 $H \rightarrow \gamma\gamma$ loop depends on κ_F and κ_V , through top and W couplings. It can be parametrized as:

$$\left| - \frac{H}{\kappa_\gamma^2} \right|^2 \sim \left| \vec{A}_F \times \frac{H}{\kappa_F} \right|^2 + \left| \vec{A}_V \times \frac{H}{\kappa_V} \right|^2$$

$$\kappa_\gamma^2 \sim 0.07 \kappa_F^2 - 0.66 \kappa_F \kappa_V + 1.59 \kappa_V^2$$

Fermion vs Vector coupling



Only the relative sign between κ_F and κ_V is physical, take $\kappa_V > 0$.

Two minima in the likelihood because of the F/V interference in the $H \rightarrow \gamma\gamma$ loop. The positive relative one is preferred by the fit but the negative relative one is allowed within 1σ

$$\kappa_F \in [-0.88, -0.75] \cup [0.73, 1.07]$$

$$\kappa_V \in [0.91, 0.97] \cup [1.05, 1.21] .$$

Fermion vs Vector

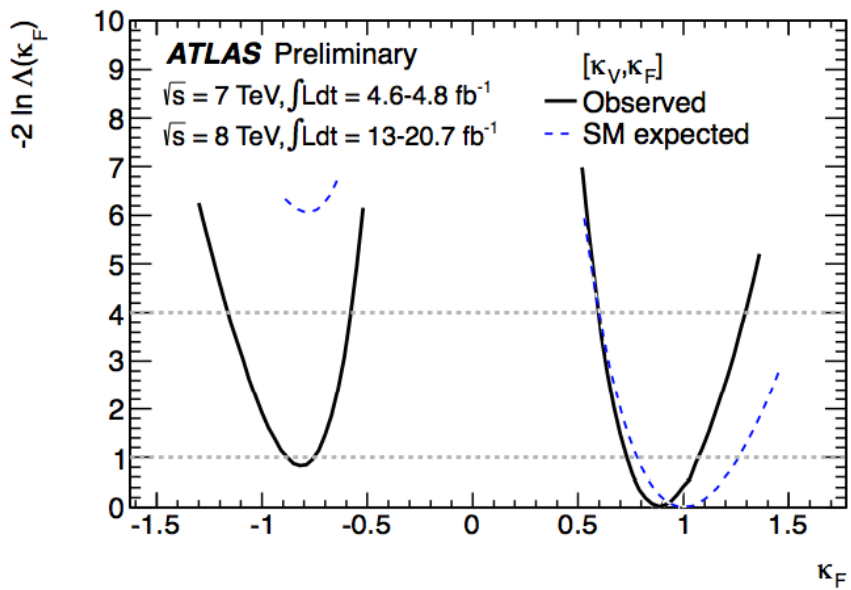
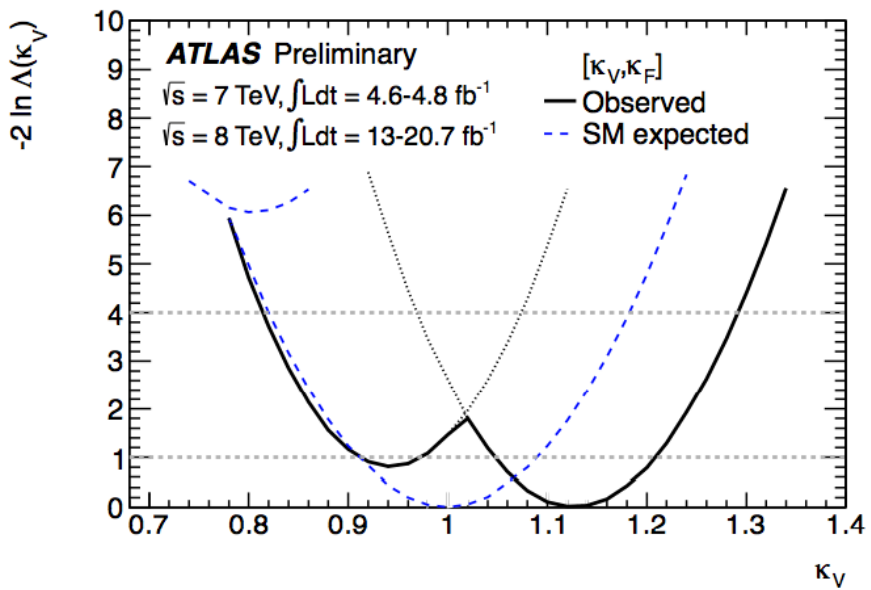
0.75 BR to fermions

and gluons

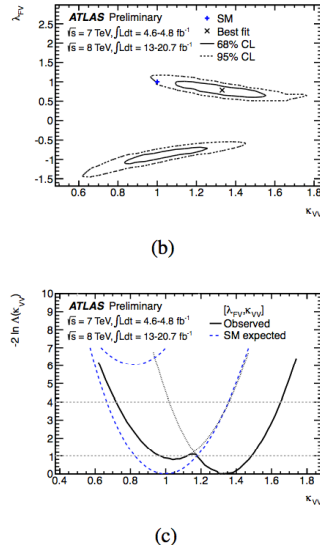
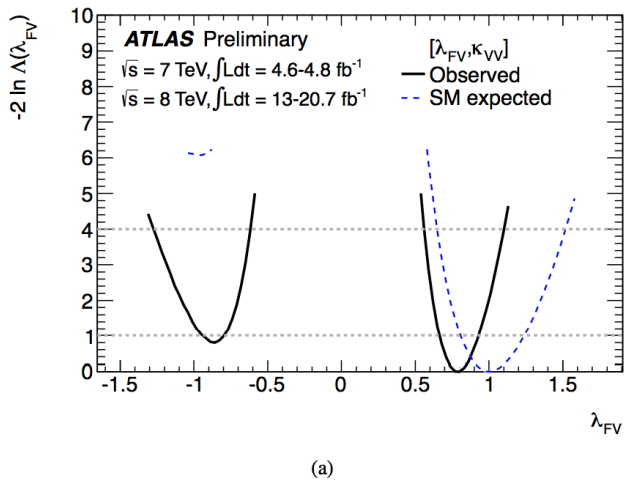
0.25 BR to $\gamma\gamma$, ZZ, WW

$$\begin{aligned}
 \sigma(gg \rightarrow H) * \text{BR}(H \rightarrow \gamma\gamma) &\sim \frac{\kappa_F^2 \cdot \kappa_\gamma^2(\kappa_F, \kappa_V)}{0.75 \cdot \kappa_F^2 + 0.25 \cdot \kappa_V^2} \\
 \sigma(qq' \rightarrow qq'H) * \text{BR}(H \rightarrow \gamma\gamma) &\sim \frac{\kappa_V^2 \cdot \kappa_\gamma^2(\kappa_F, \kappa_V)}{0.75 \cdot \kappa_F^2 + 0.25 \cdot \kappa_V^2} \\
 \sigma(gg \rightarrow H) * \text{BR}(H \rightarrow ZZ^{(*)}, H \rightarrow WW^{(*)}) &\sim \frac{\kappa_F^2 \cdot \kappa_V^2}{0.75 \cdot \kappa_F^2 + 0.25 \cdot \kappa_V^2} \\
 \sigma(qq' \rightarrow qq'H) * \text{BR}(H \rightarrow ZZ^{(*)}, H \rightarrow WW^{(*)}) &\sim \frac{\kappa_V^2 \cdot \kappa_V^2}{0.75 \cdot \kappa_F^2 + 0.25 \cdot \kappa_V^2} \\
 \sigma(qq' \rightarrow qq'H, VH) * \text{BR}(H \rightarrow \tau\tau, H \rightarrow b\bar{b}) &\sim \frac{\kappa_V^2 \cdot \kappa_F^2}{0.75 \cdot \kappa_F^2 + 0.25 \cdot \kappa_V^2}
 \end{aligned}$$

$$\kappa_\gamma^2(\kappa_F, \kappa_V) = 1.59 \cdot \kappa_V^2 - 0.66 \cdot \kappa_V \kappa_F + 0.07 \cdot \kappa_F^2$$



Fermion vs Vector (no assumption on the total width)

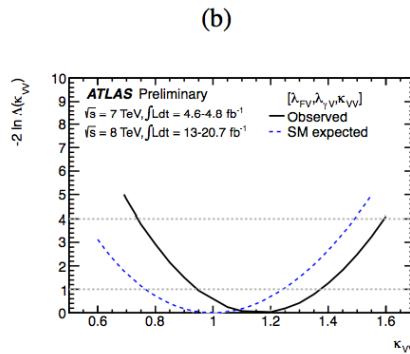
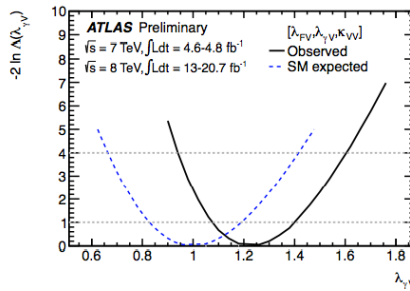
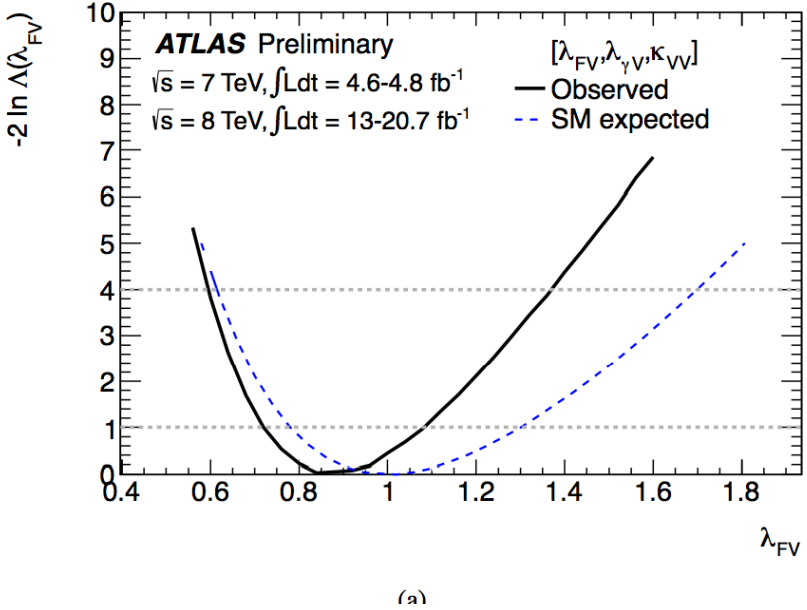


$$\lambda_{FV} = \kappa_F / \kappa_V$$

$$\kappa_{VV} = \kappa_V \cdot \kappa_V / \kappa_H$$

$$\begin{aligned}
 \sigma(gg \rightarrow H) * \text{BR}(H \rightarrow \gamma\gamma) &\sim \lambda_{FV}^2 \cdot \kappa_{VV}^2 \cdot \kappa_\gamma^2(\lambda_{FV}, 1) \\
 \sigma(qq' \rightarrow qq'H) * \text{BR}(H \rightarrow \gamma\gamma) &\sim \kappa_{VV}^2 \cdot \kappa_\gamma^2(\lambda_{FV}, 1) \\
 \sigma(gg \rightarrow H) * \text{BR}(H \rightarrow ZZ^{(*)}, H \rightarrow WW^{(*)}) &\sim \lambda_{FV}^2 \cdot \kappa_{VV}^2 \\
 \sigma(qq' \rightarrow qq'H) * \text{BR}(H \rightarrow ZZ^{(*)}, H \rightarrow WW^{(*)}) &\sim \kappa_{VV}^2 \\
 \sigma(qq' \rightarrow qq'H, VH) * \text{BR}(H \rightarrow \tau\tau, H \rightarrow b\bar{b}) &\sim \kappa_{VV}^2 \cdot \lambda_{FV}^2 ,
 \end{aligned}$$

Fermion vs Vector (no assumptions)



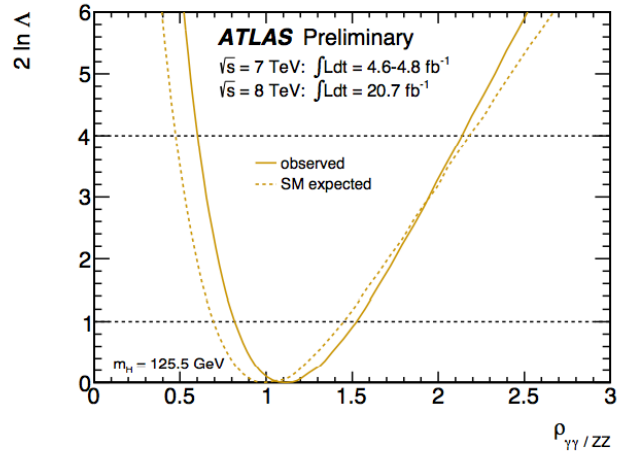
$$\begin{aligned}\lambda_{FV} &= \kappa_F / \kappa_V \\ \lambda_{\gamma V} &= \kappa_\gamma / \kappa_V \\ \kappa_{VV} &= \kappa_V \cdot \kappa_V / \kappa_H \quad ,\end{aligned}$$

$$\begin{aligned}\sigma(gg \rightarrow H) * \text{BR}(H \rightarrow \gamma\gamma) &\sim \lambda_{FV}^2 \cdot \kappa_{VV}^2 \cdot \lambda_{\gamma V}^2 \\ \sigma(qq' \rightarrow qq'H) * \text{BR}(H \rightarrow \gamma\gamma) &\sim \kappa_{VV}^2 \cdot \lambda_{\gamma V}^2 \\ \sigma(gg \rightarrow H) * \text{BR}(H \rightarrow ZZ^{(*)}, H \rightarrow WW^{(*)}) &\sim \lambda_{FV}^2 \cdot \kappa_{VV}^2 \\ \sigma(qq' \rightarrow qq'H) * \text{BR}(H \rightarrow ZZ^{(*)}, H \rightarrow WW^{(*)}) &\sim \kappa_{VV}^2 \\ \sigma(qq' \rightarrow qq'H, VH) * \text{BR}(H \rightarrow \tau\tau, H \rightarrow b\bar{b}) &\sim \kappa_{VV}^2 \cdot \lambda_{FV}^2 \quad .\end{aligned}$$

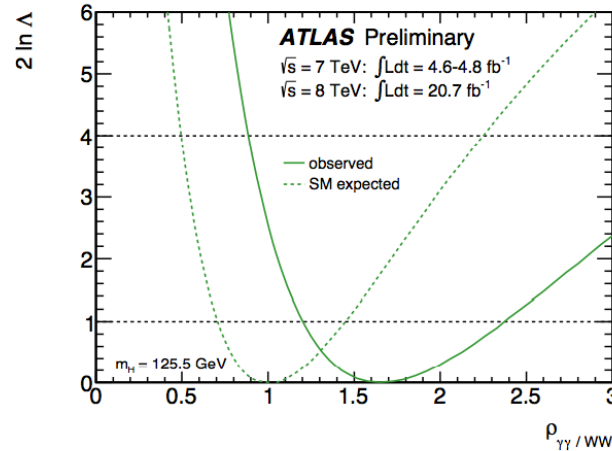
The non-vanishing value of the fitted coupling of the new particle to gauge bosons κ_V is both directly and indirectly constrained by several channels at the $\sim 20\%$ level. The coupling to fermions can be directly observed in the $H \rightarrow \tau\tau$ and $H \rightarrow b\bar{b}$ channels. However, this direct constraint is weak as both channels are compatible with both the SM Higgs boson signal and the SM background hypothesis at the 95% CL level (see Fig. 1). A value of κ_F significantly deviating from zero is indirectly observed through the constraints from the channels which are dominated by the main production process $gg \rightarrow H$, which is assumed to be fermion mediated in this benchmark model.

The ratio between the fermion and vector coupling λ_{FV} is compatible with the SM hypothesis, independently of the inclusion of the $H \rightarrow \gamma\gamma$ channel in the measurement of the λ_{FV} ratio.

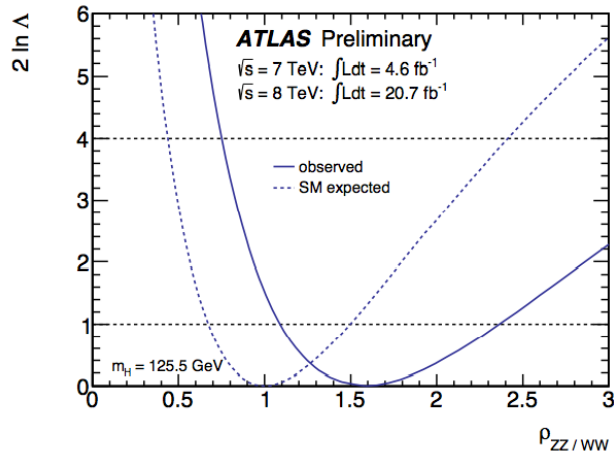
Decay modes



(a)



(b)



$$\begin{aligned}\rho_{\gamma\gamma/ZZ} &= 1.1^{+0.4}_{-0.3} \\ \rho_{\gamma\gamma/WW} &= 1.7^{+0.7}_{-0.5} \\ \rho_{ZZ/WW} &= 1.6^{+0.8}_{-0.5}\end{aligned}$$